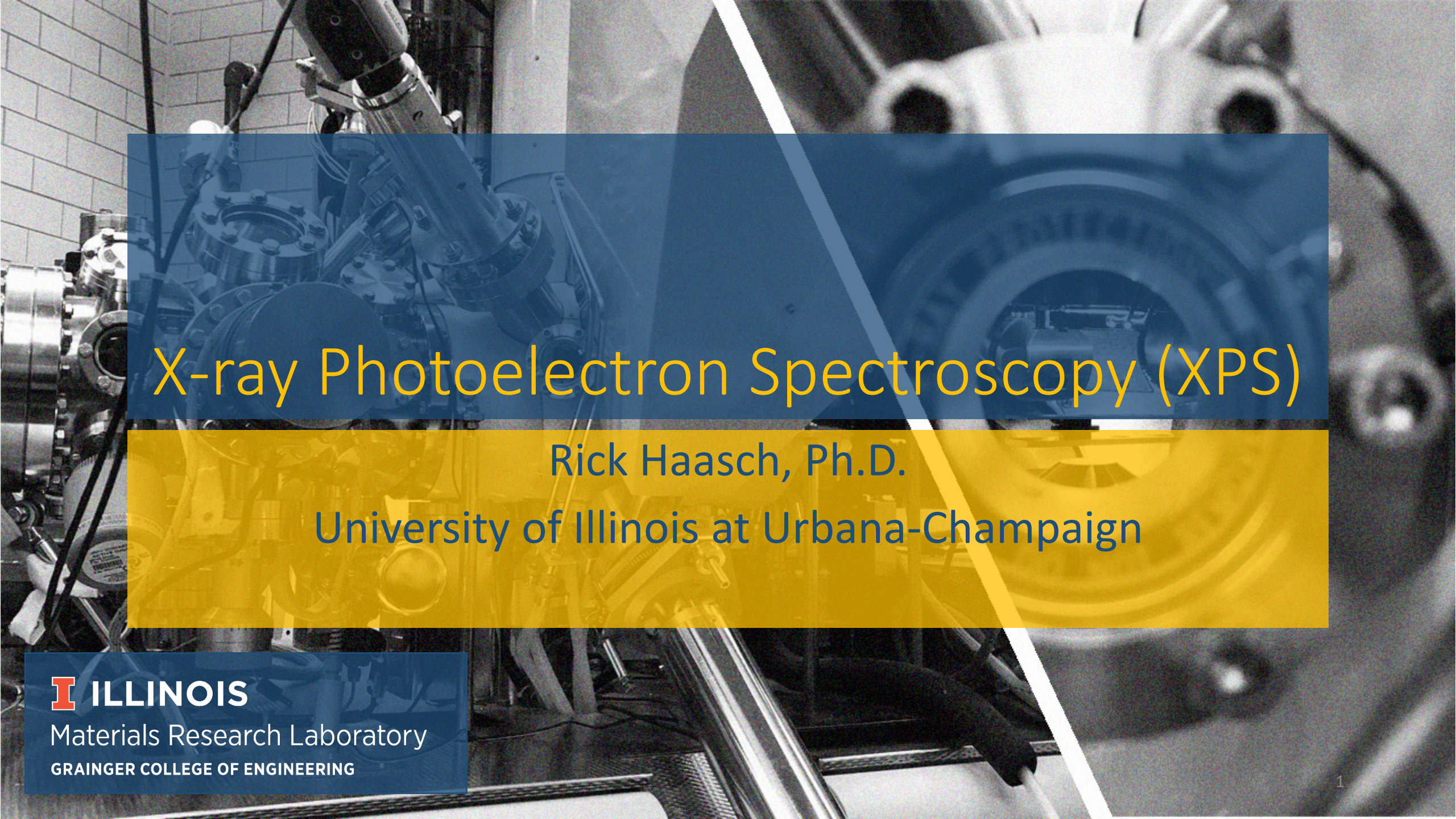

X-ray Photoelectron Spectroscopy (XPS)

Rick Haasch, Ph.D.

University of Illinois at Urbana-Champaign

ILLINOIS
Materials Research Laboratory
GRAINGER COLLEGE OF ENGINEERING

Surfaces and Interfaces

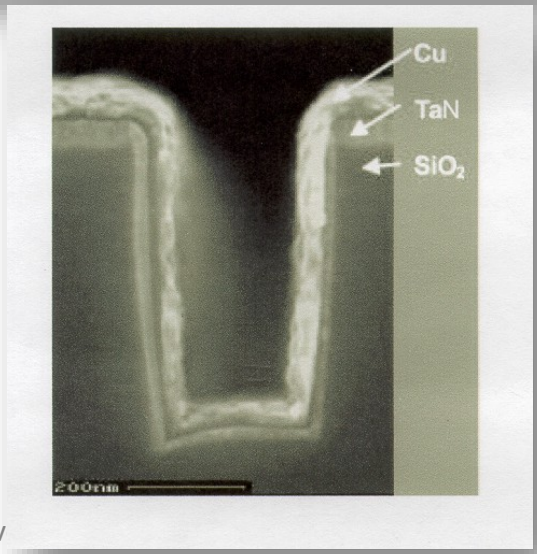

High-power Lithium-ion Battery

The Electrochemical Society
Advancing solid state & electrochemical science & technology

DONATE

ABOUT ECS | MEMBERSHIP | PUBLICATIONS | PROGRAMS | MEETINGS

ECSblog ecsblog.org

HOME / SUSTAINABILITY SCIENCE / BATTERIES / DAHN UNVEILS MILLION MILE BATTERY IN GROUND-BREAKING ARTICLE

Previous Post Next Post

EMAIL SIGN UP

Dahn Unveils Million Mile Battery in Ground-breaking Article

Posted on September 25, 2019 by Frances Chaves

Elon Musk promised—and Jeff Dahn delivered! With the publishing of a ground-breaking paper in the *Journal of The Electrochemical Society* (JES), Dahn announced to the world that Tesla may soon have a battery that makes their robot taxis and long-haul electric trucks viable. Dahn and his research group is Tesla's battery research partner. Dahn says "… that cells of this type should be able to power an electric vehicle for over one million miles and last at least two decades in grid energy storage."

According to Doron Aurbach, JES batteries and energy storage technical editor, "This comprehensive article is expected to be impactful in the field of batteries and energy storage. It is a very systematic study by one of the most renowned and prestigious electrochemistry groups in the world. It was a pleasure for me as a technical editor to handle this paper. It substantiates all the statements about the truly high quality and importance of JES, one of the leading and most prestigious journals in electrochemistry.

“God made the bulk; the surface was invented by the devil.”

— Wolfgang Pauli

“The best that most of us can hope to achieve in physics is simply to misunderstand at a deeper level.”

— Wolfgang Pauli

Particle Surface Interactions

Primary beam
(source)

Ions
Electrons
Photons

Secondary beam
(spectrometers, detectors)

Ions
Electrons
Photons

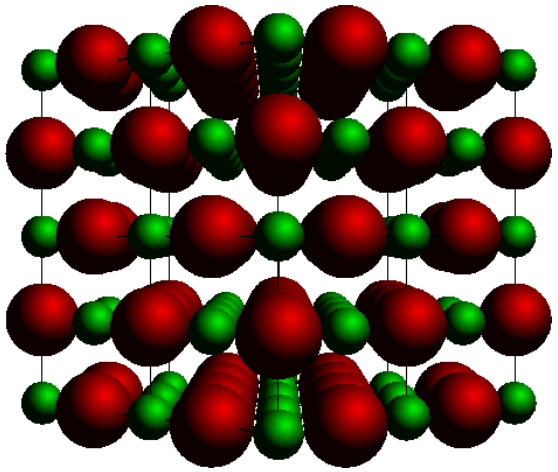

What is the Surface?

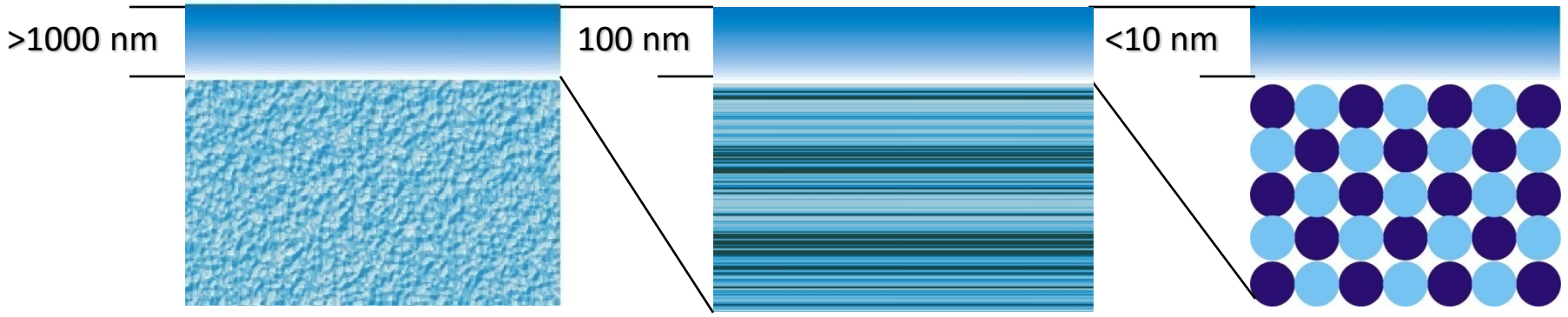

Bulk Analysis **Thin-film Analysis** **Surface Analysis**

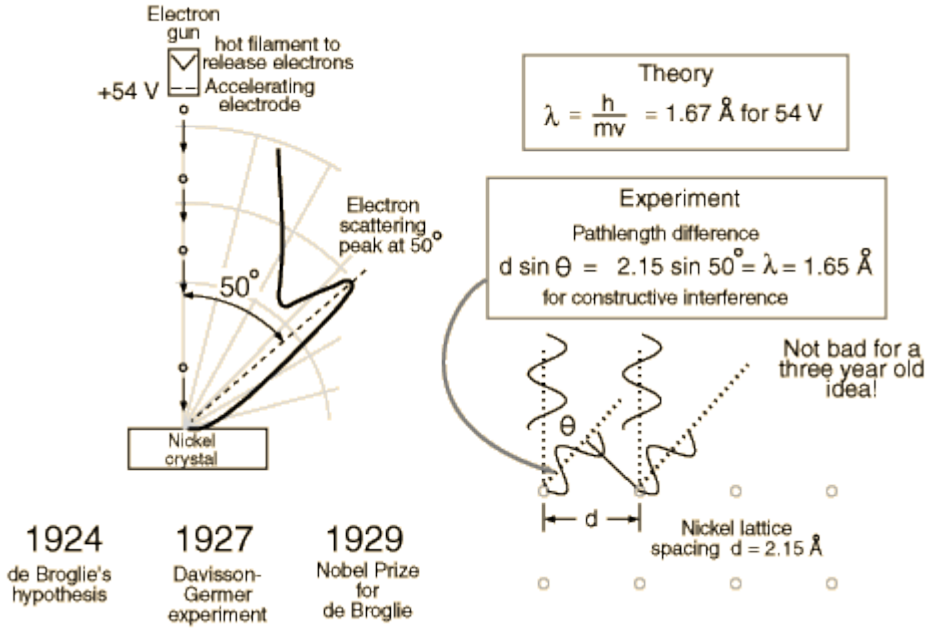

For an electron with **KE = 1 eV** and rest mass energy of 0.511 MeV, the de Broglie wavelength is **1.23 nm** (~1000X less than a 1 eV photon).

http://hyperphysics.phy-astr.gsu.edu/hbase/davger.html#c1

Particle Surface Interactions

Photoelectron Spectroscopy

Ions
Electrons
Photons

Ions
Electrons
Photons

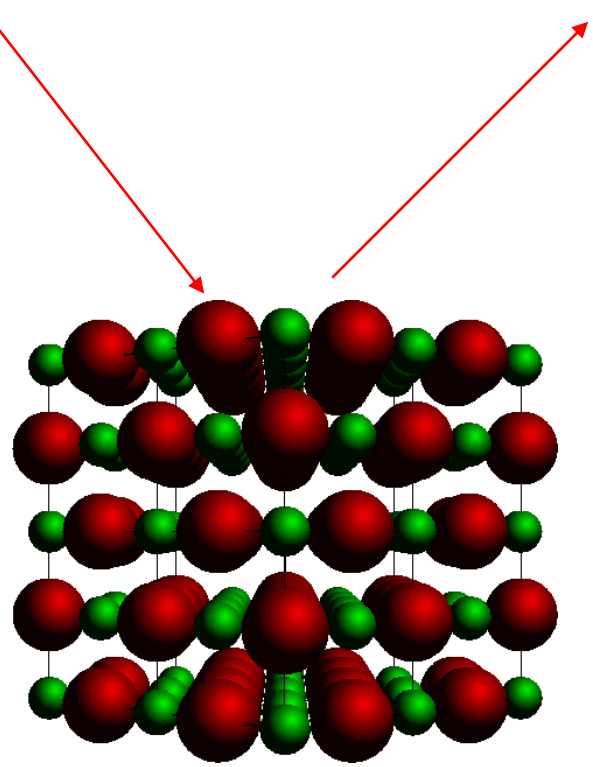

Vacuum

X-ray Photoelectron Spectroscopy (XPS)

X-ray Photoelectron Spectroscopy (XPS), also known as **Electron Spectroscopy for Chemical Analysis (ESCA)** is a widely used technique to investigate the chemical composition of surfaces.

X-ray[1] Photoelectron spectroscopy, based on the photoelectric effect,[2,3] was developed in the mid-1960's as a practical technique by Kai Siegbahn and his research group at the University of Uppsala, Sweden.[4]

Wilhelm Conrad Röntgen

Heinrich Rudolf Hertz

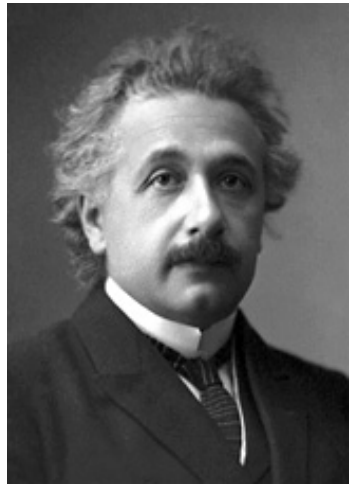

Albert Einstein

Kai M. Siegbahn

1. W. Röntgen, 1901 Nobel Prize in Physics "in recognition of the extraordinary services he has rendered by the discovery of the remarkable rays subsequently named after him."
2. H. Hertz, "*Über einen Einfluss des ultravioletten Lichtes auf die electrische Entladung," Ann. Physik* **31**,983 (1887). The IEEE Heinrich Hertz Medal was established by the Board of Directors in 1987 "for outstanding achievements in Hertzian (radio) waves."
3. A. Einstein, "*Über einen die Erzeugung und Verwandlung des Lichtes betreffenden heuristischen Gesichtspunkt," Ann. Physik* **17**,132 (1905). 1921 Nobel Prize in Physics "for his services to Theoretical Physics, and especially for his discovery of the law of the photoelectric effect."
4. 4. K. Siegbahn, Et. Al.,*Nova Acta Regiae Soc.Sci.,* Ser. IV, Vol. 20 (1967). 1981 Nobel Prize in Physics "for his contribution to the development of high resolution electron spectroscopy."

X-ray Photoelectron Spectroscopy Small Area Detection

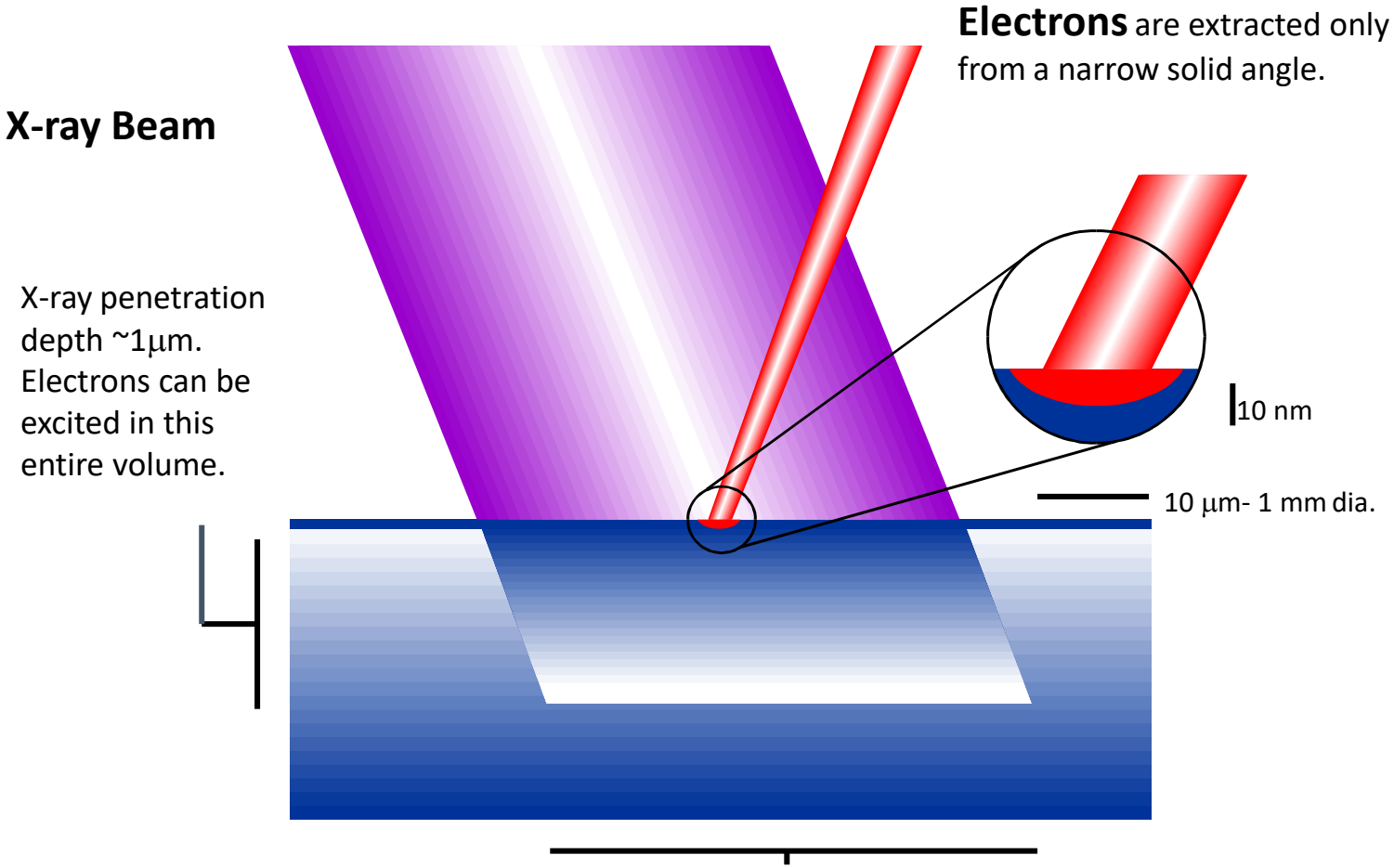

Photoelectron and Auger Electron Emission

KE (measured) = ***hν*** (known) - **BE** - Φ_{spec} (calibrated)

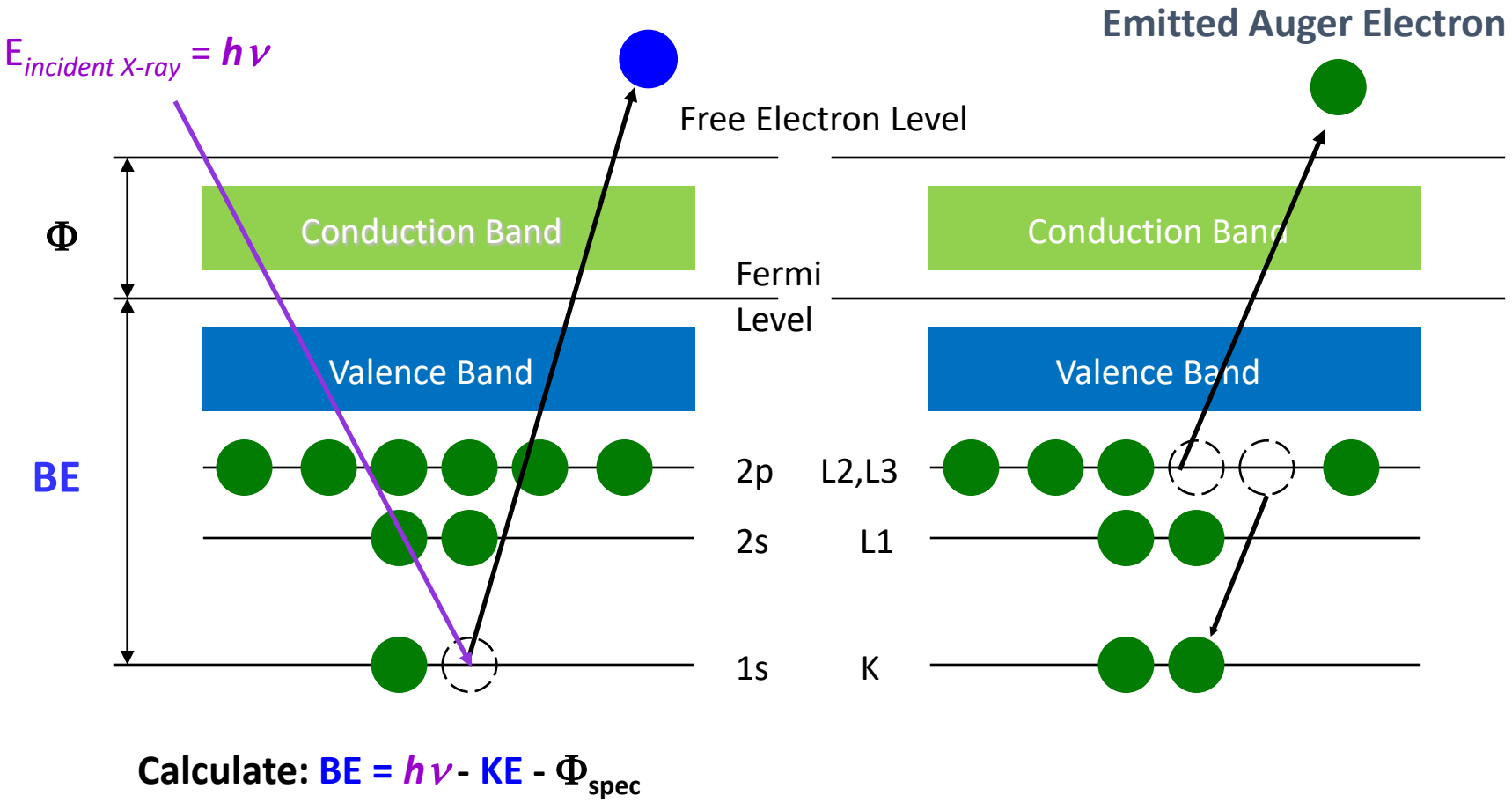

Calculate: BE = *hν* - KE - Φ_{spec}

BE – binding energy depends on Z, i.e. characteristic for the element

Photoelectron and Auger Electron Emission

KE (measured) = ***hν*** (known) - **BE** - Φ_{spec} (calibrated)

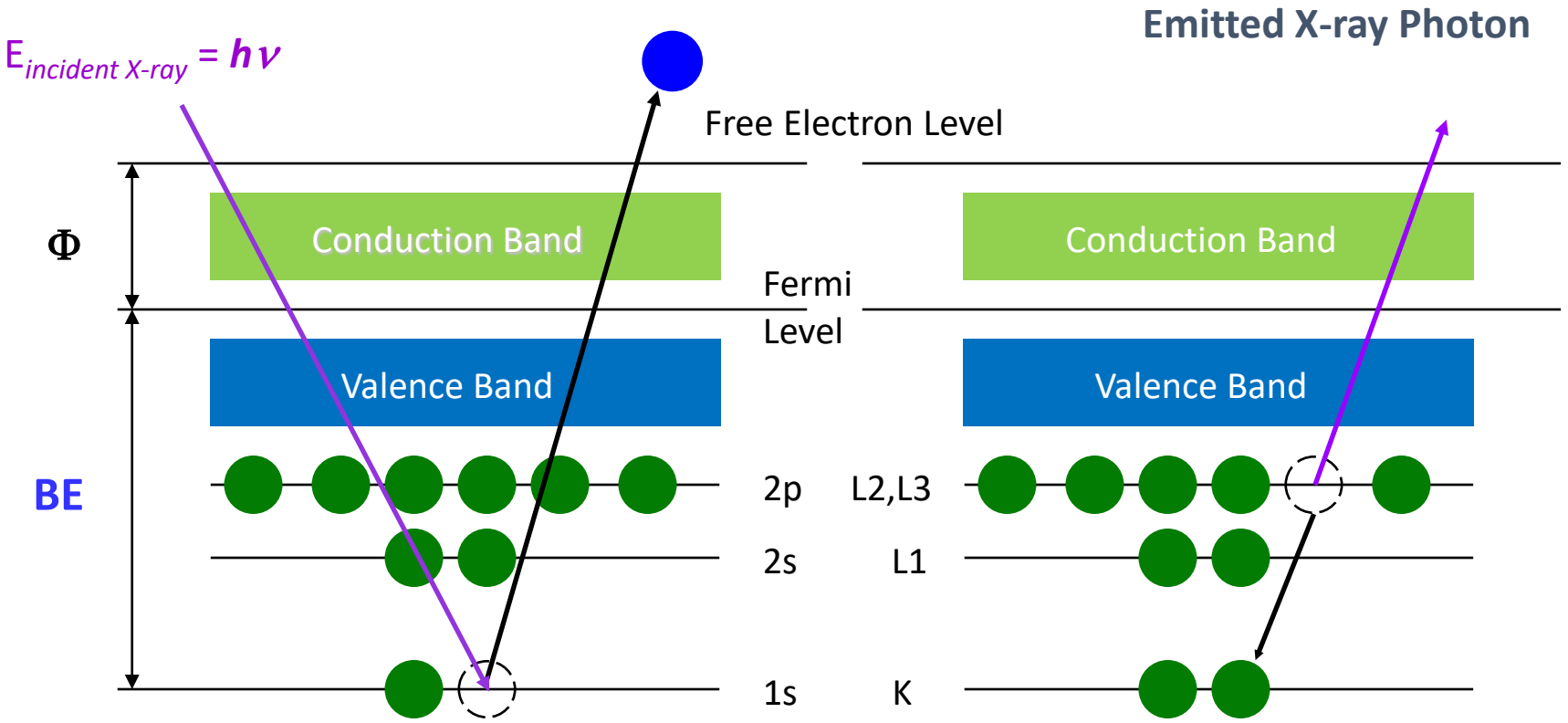

Calculate: BE = *hν* - KE - Φ_{spec}

BE – binding energy depends on Z, i.e. characteristic for the element

Photoelectron and Auger Electron Emission

Photoelectron and Auger Electron Emission

Photoelectron and Auger Electron Emission

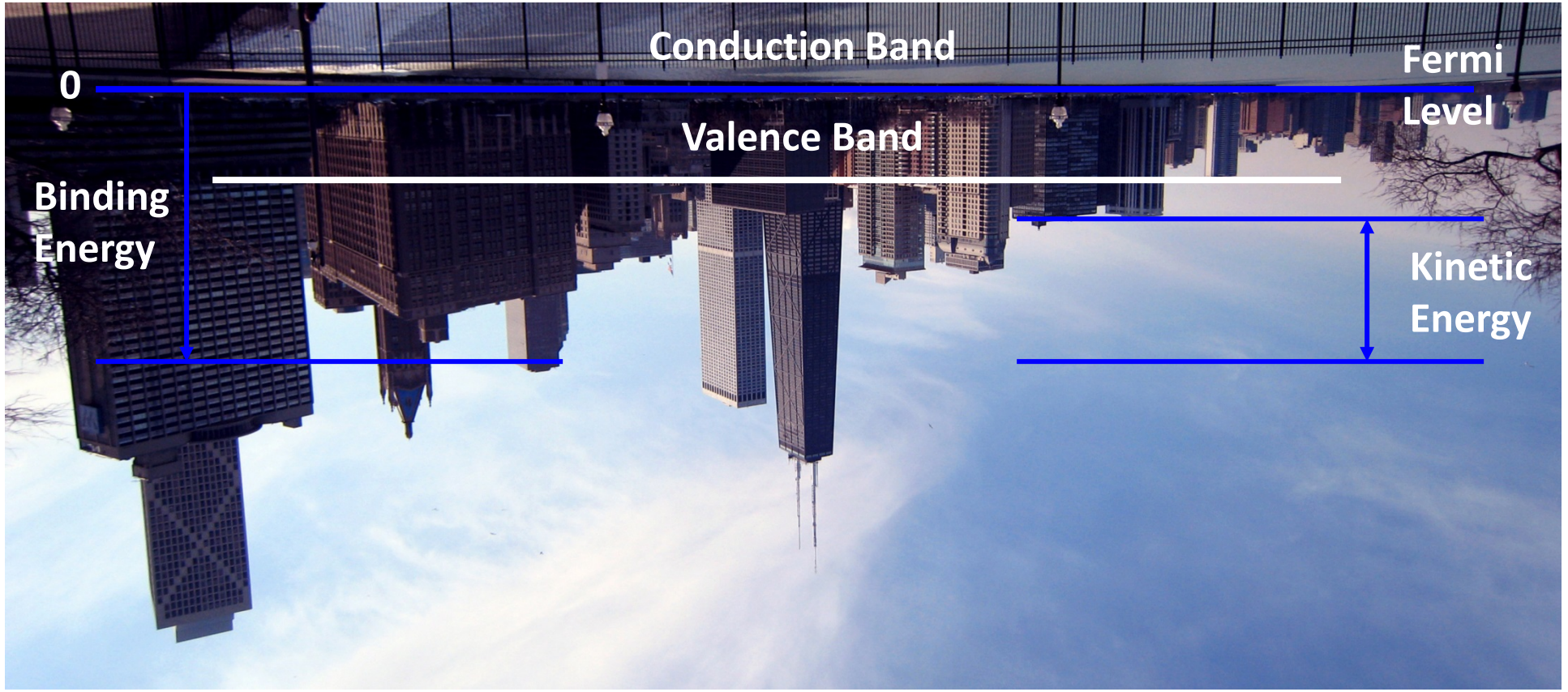

Photoelectron Lines

Auger Electron Lines

Photoelectron and Auger Electron Emission

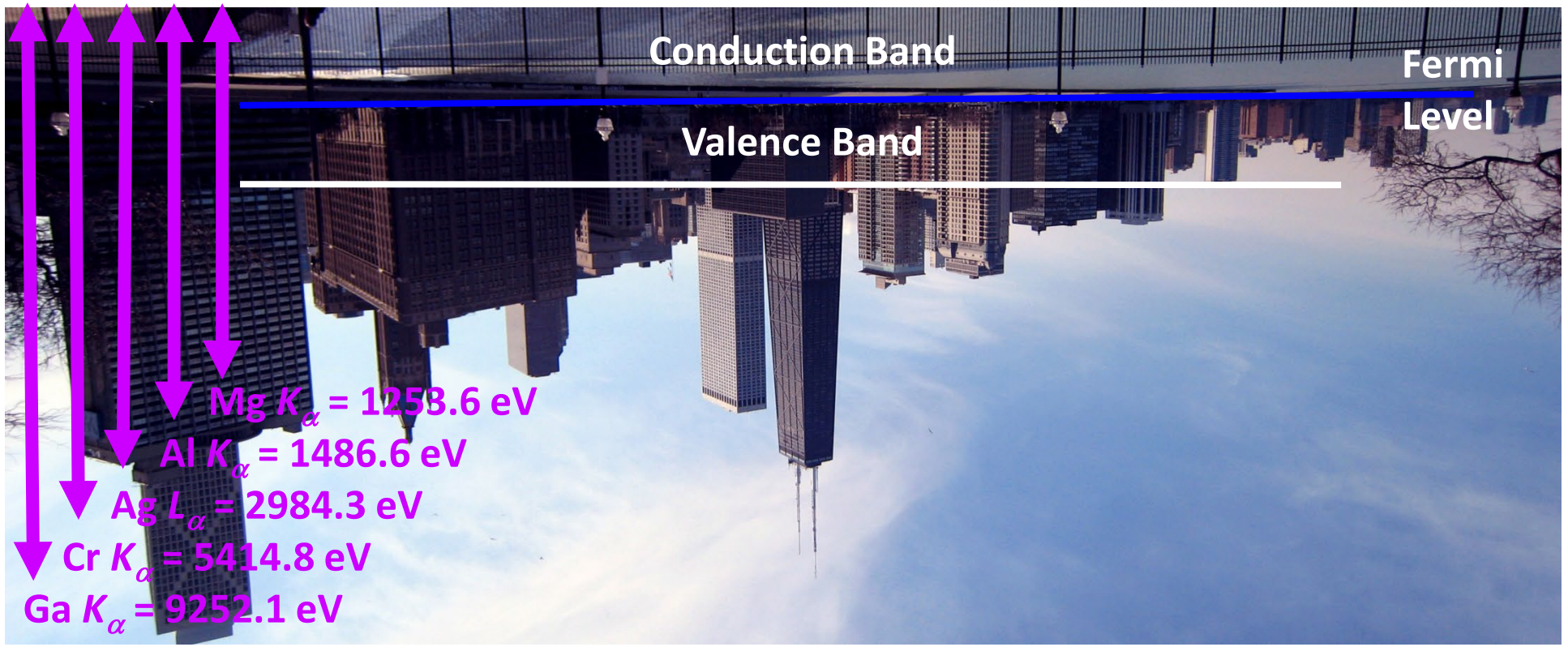

XPS can probe all of the orbitals in only the light elements.

***e.g.* BE C 1s = 285 eV, Mg 1s =1304 eV, Au 1s ≈ 81000 eV**

Surface Sensitivity: Electron Spectroscopy

Inelastic Mean-Free Path: The mean distance an electron can travel between inelastic scattering events.

Inelastic mean-free paths (calculated) based on TPP-2M*

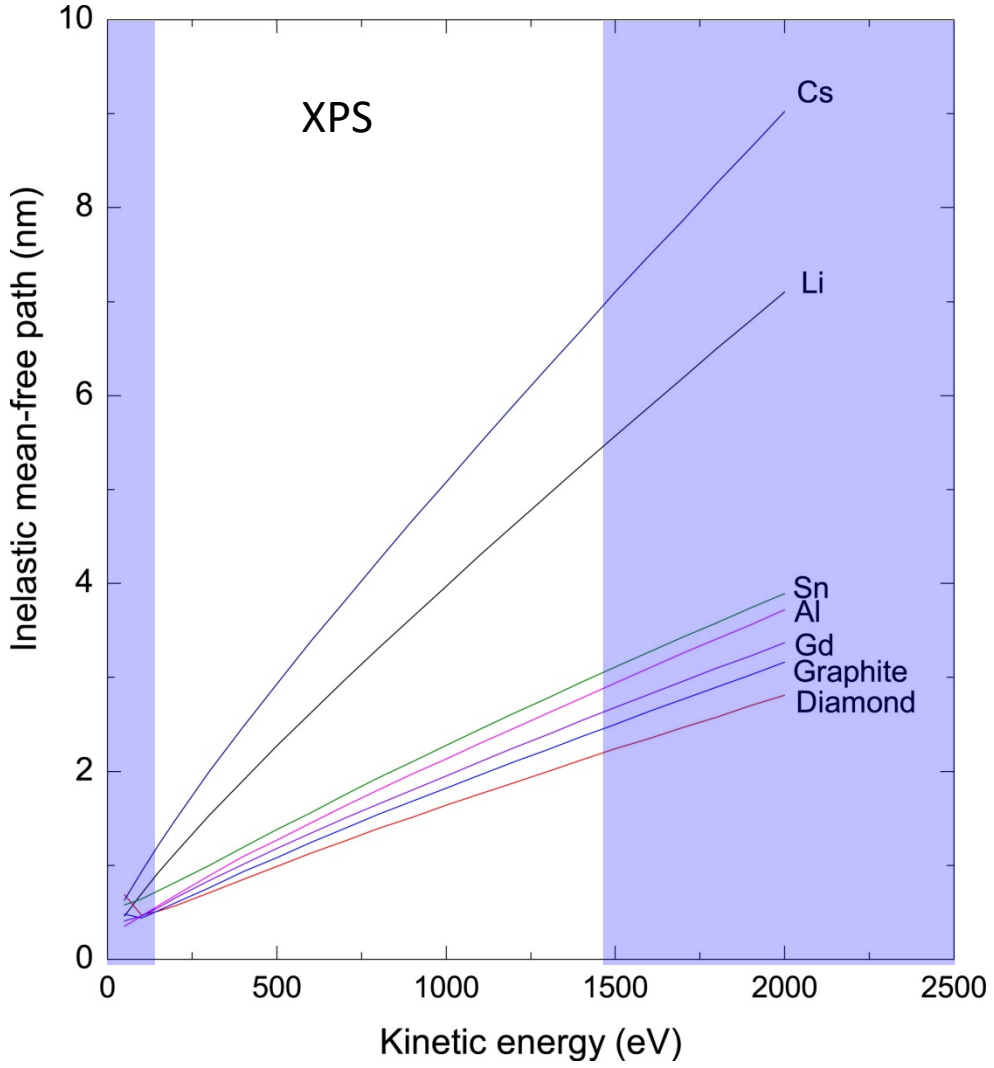

Electrons travel only a few nanometers through solids.

*S. Tanuma, C. J. Powell, D. R. Penn, *Surface and Interface Analysis*, **36**, 1 (2004).

Surface Sensitivity: Electron Spectroscopy

Assuming Inelastic Scattering Only

Beer-Lambert relationship:

$I = I_0 \exp(-d/\lambda \cos\theta)$

where d = depth

λ = Inelastic mean free path

at 3λ, $I/I_0 = 0.05$

at 1000 eV, $\lambda \approx 1.6$ nm

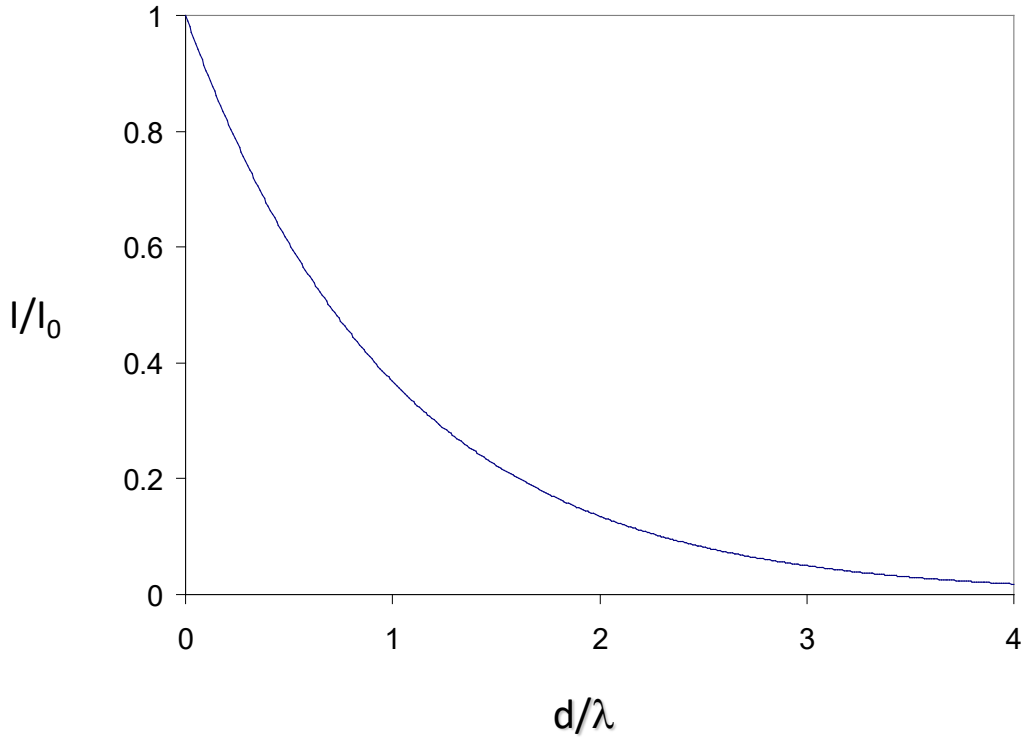

95% of the signal comes from within 5 nm of the surface or less!


Ratio: 100
Mt. Hood Prominence: 7707 feet
Douglas Fir Height: ~77 feet
Ratio: 10000
Fingerprint Residue: ~50000 nm
XPS Sensitivity: ~5 nm

Surface Sensitivity: Electron Spectroscopy

X-ray Photoelectron Spectroscopy

Advantage

Extremely surface sensitive!

Disadvantage

Extremely surface sensitive!

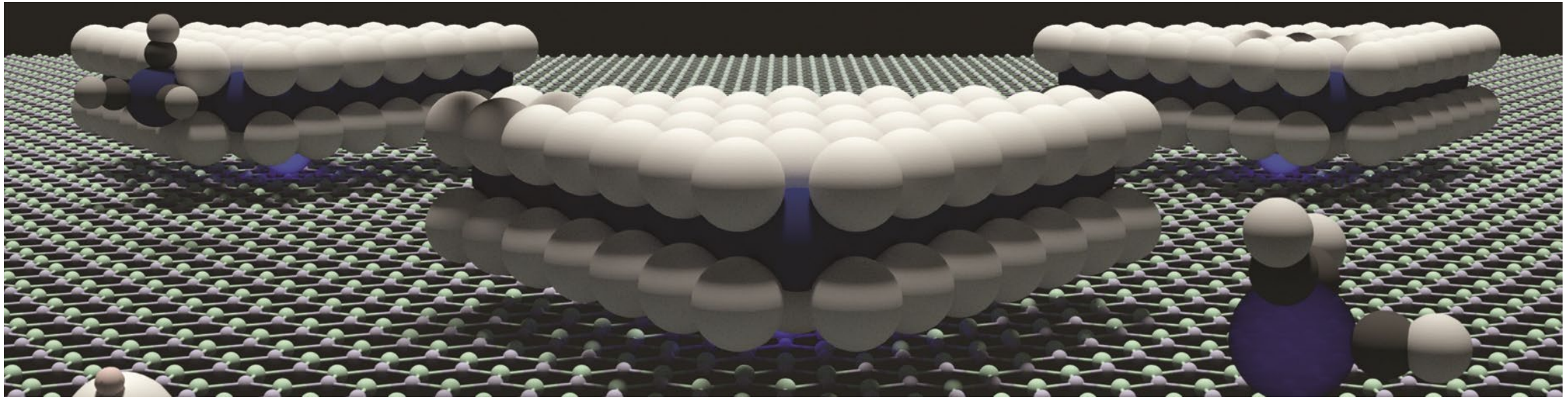

https://phys.org/news/2019-05-substrate-defects-key-growth-d.html

Ion Sputtering

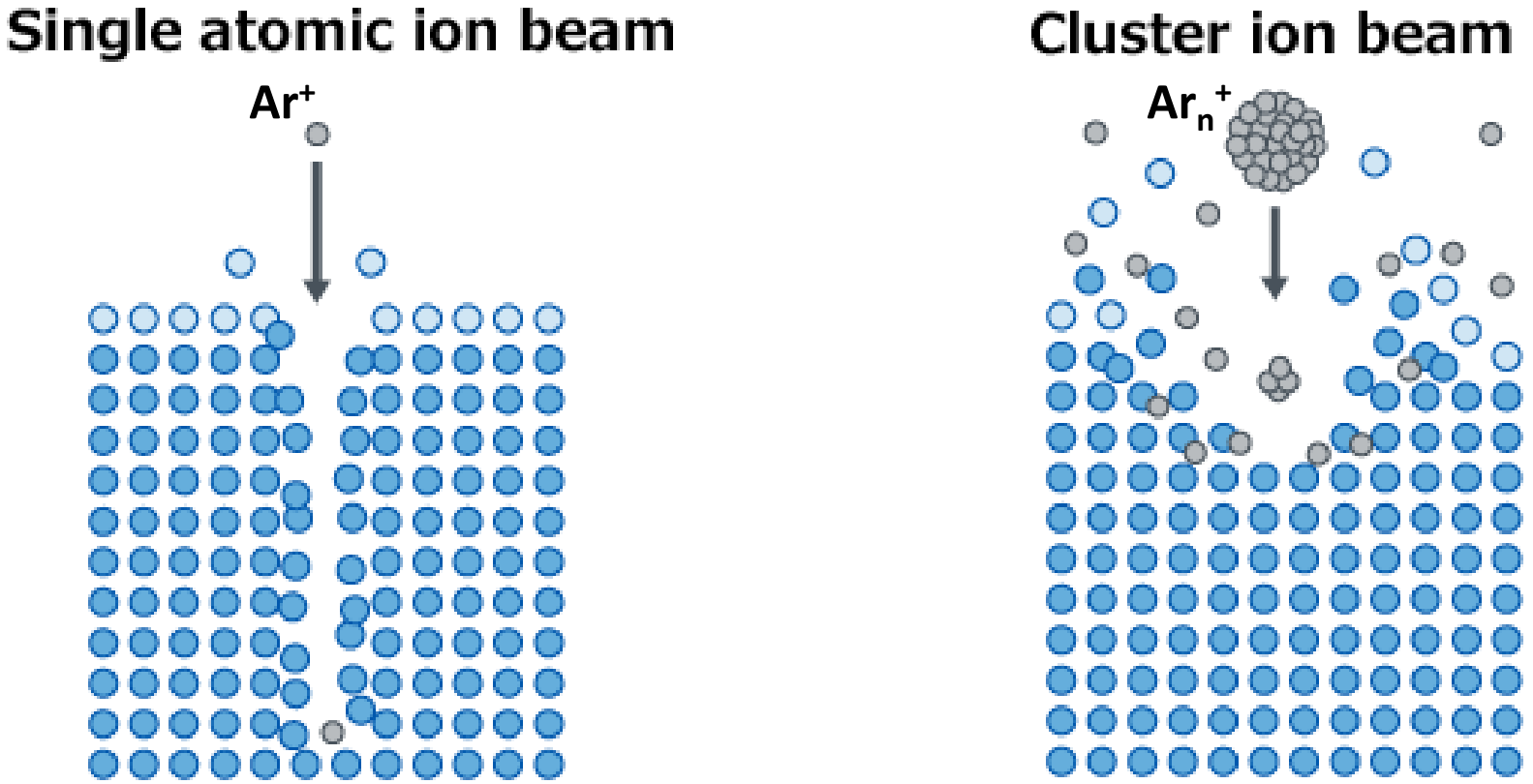

- Ions striking a surface interact with atoms in a series collisions.
- recoiled target atoms in turn collide with atom at rest generating a collision cascade.
- The initial ion energy and momentum are distributed among the target recoil atoms.
- When E_i > 1 keV, the cascade is "linear," *i.e.* approximated by a series of binary collisions in a stationary matrix.

P. Sigmund, "Sputtering by ion bombardment: theoretical concepts," in *Sputtering by particle bombardment I*, edited by R. Behrish, Springer-Verlag, 1981.
Image credit: https://ulvac-phi.com/

15 KeV Ga^+

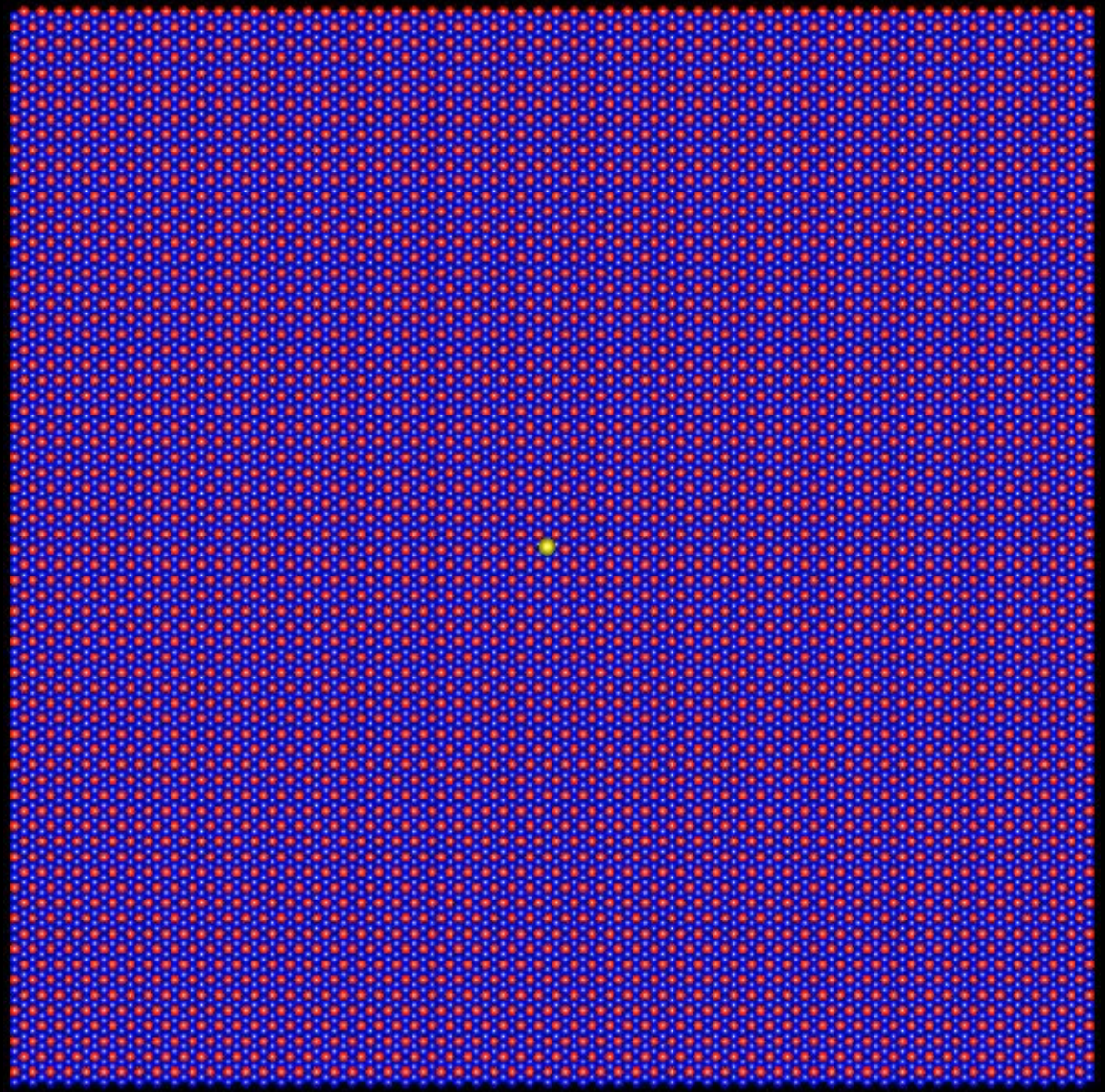

15 KeV C_{60}^+

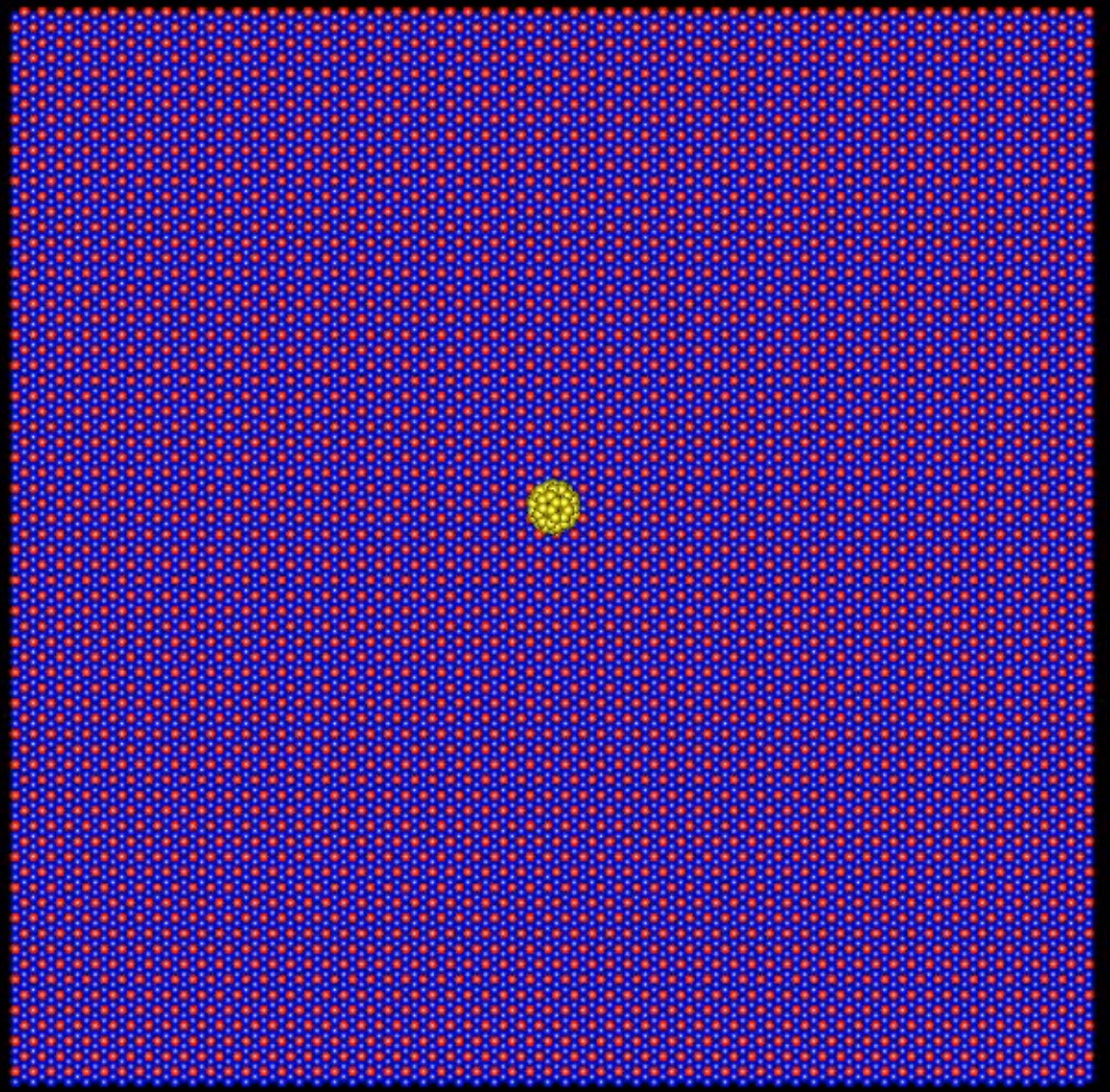

Sputtering animations and review articles (psu.edu): https://garrison.chem.psu.edu/research/classic-sputtering-animations-and-review-papers/

X-ray Photoelectron Spectrometer

1. Spherical mirror analyser
2. Hemispherical analyser
3. Delay-line detector
4. Electrostatic lens
5. Selected area aperture drive
6. Octopole scan plates
7. Variable iris drive
8. Charge neutraliser
9. Magnetic lens

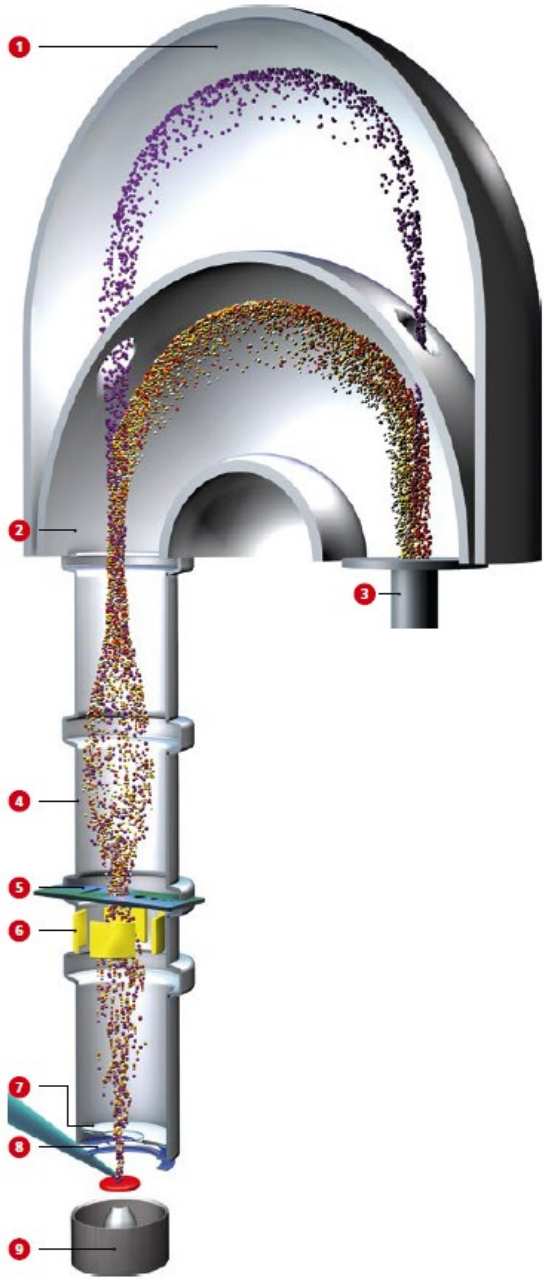

Image credit: https://www.kratos.com/

Gas-cluster Ion Source (GCIS)

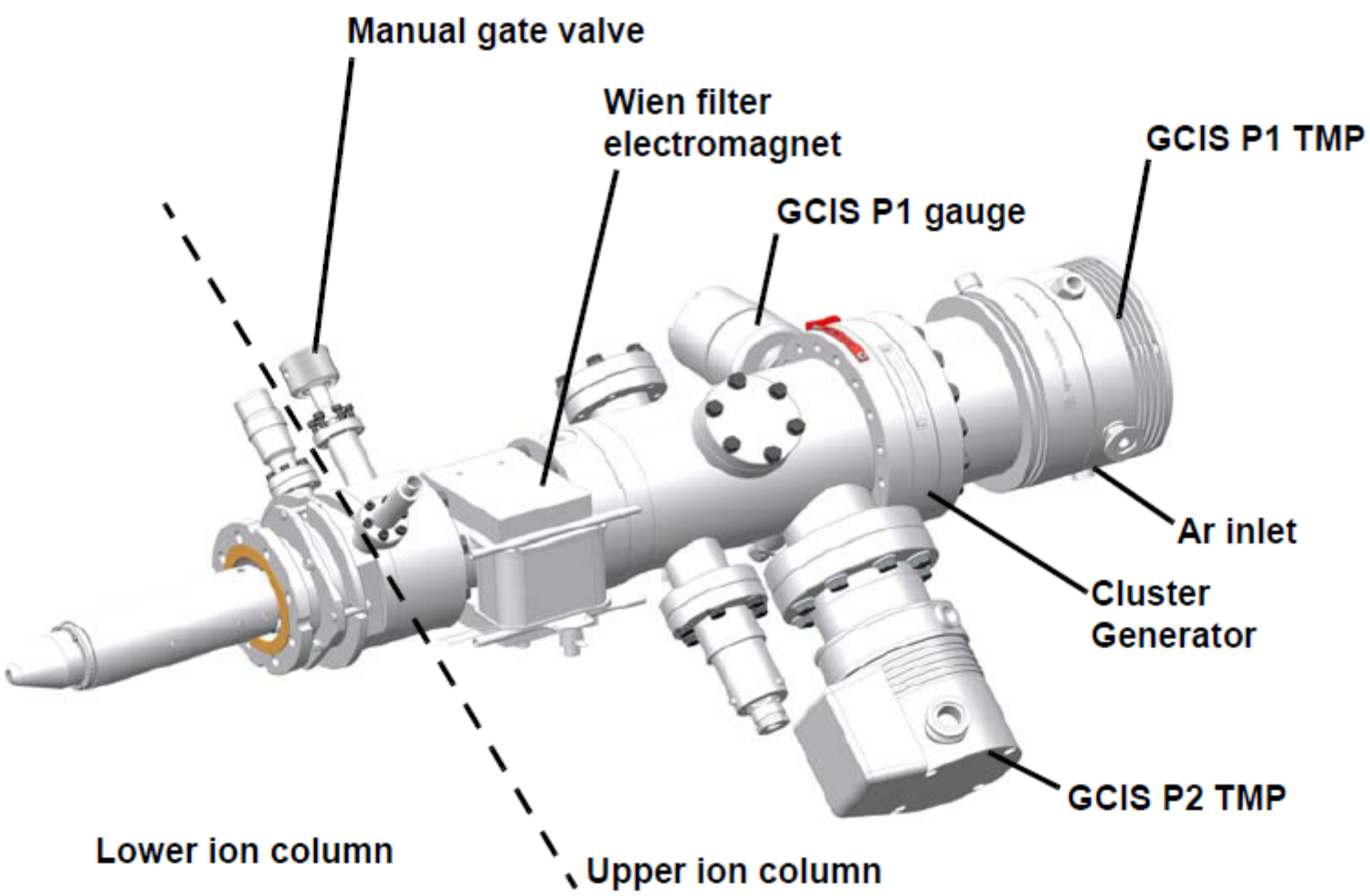

Elemental Shifts

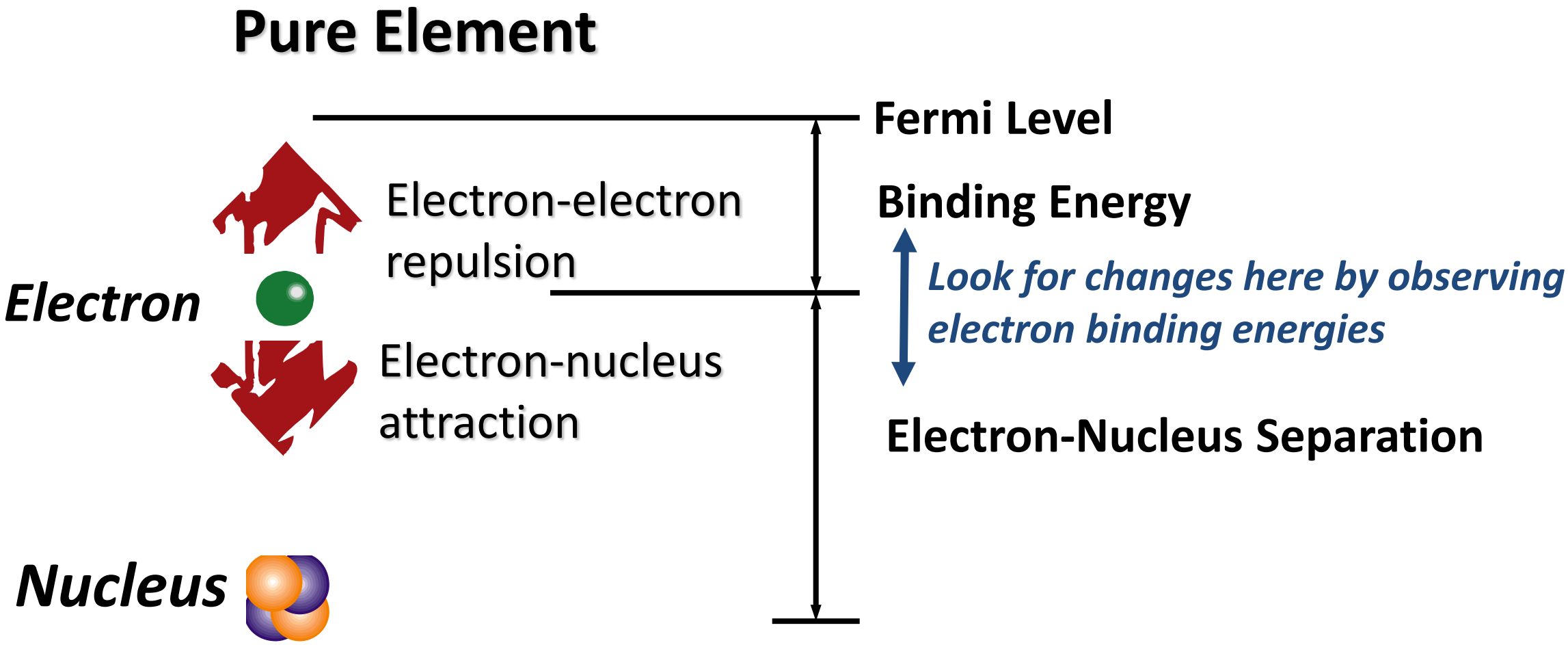

Elemental Shifts

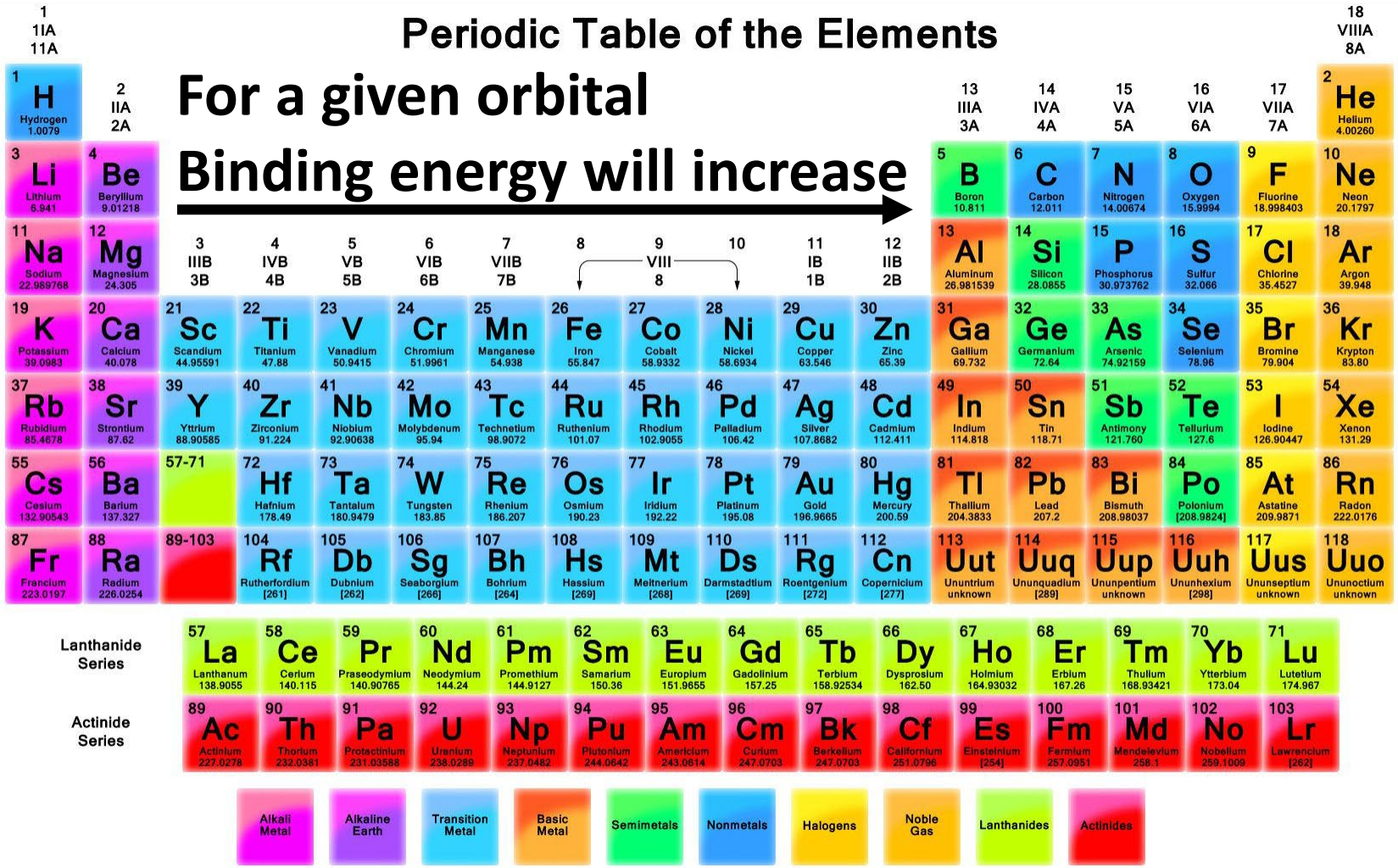

©okiraa.com

Elemental Shifts

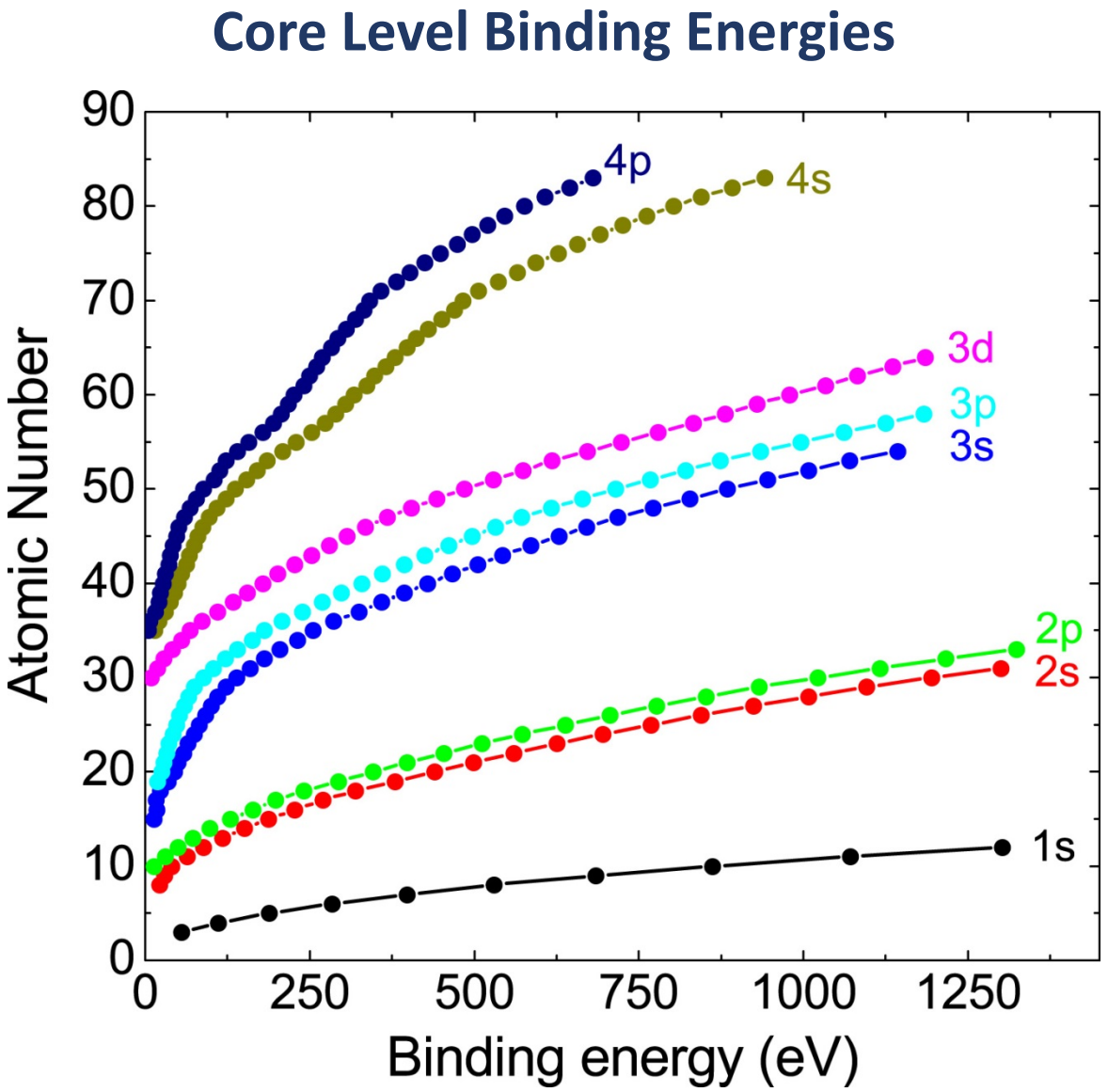

Elemental Shifts – Higher Energy X-ray Sources

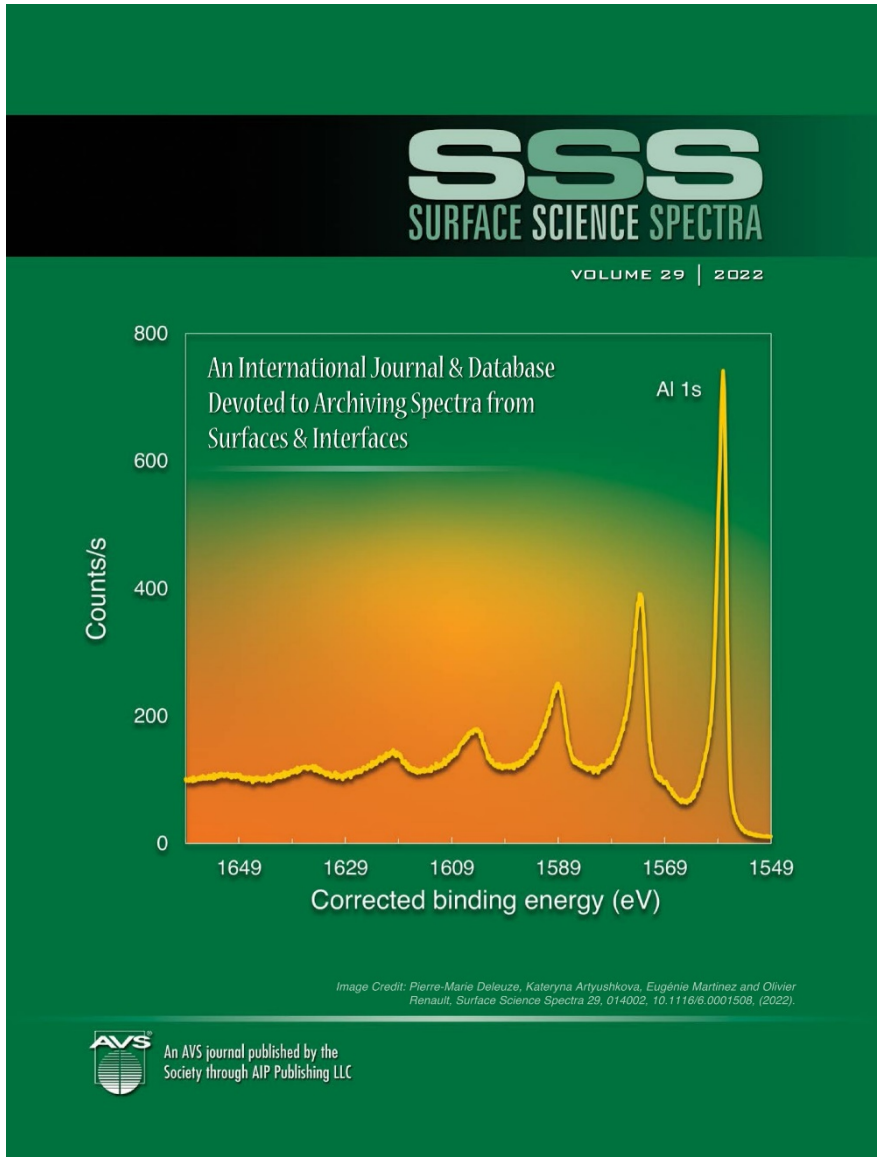

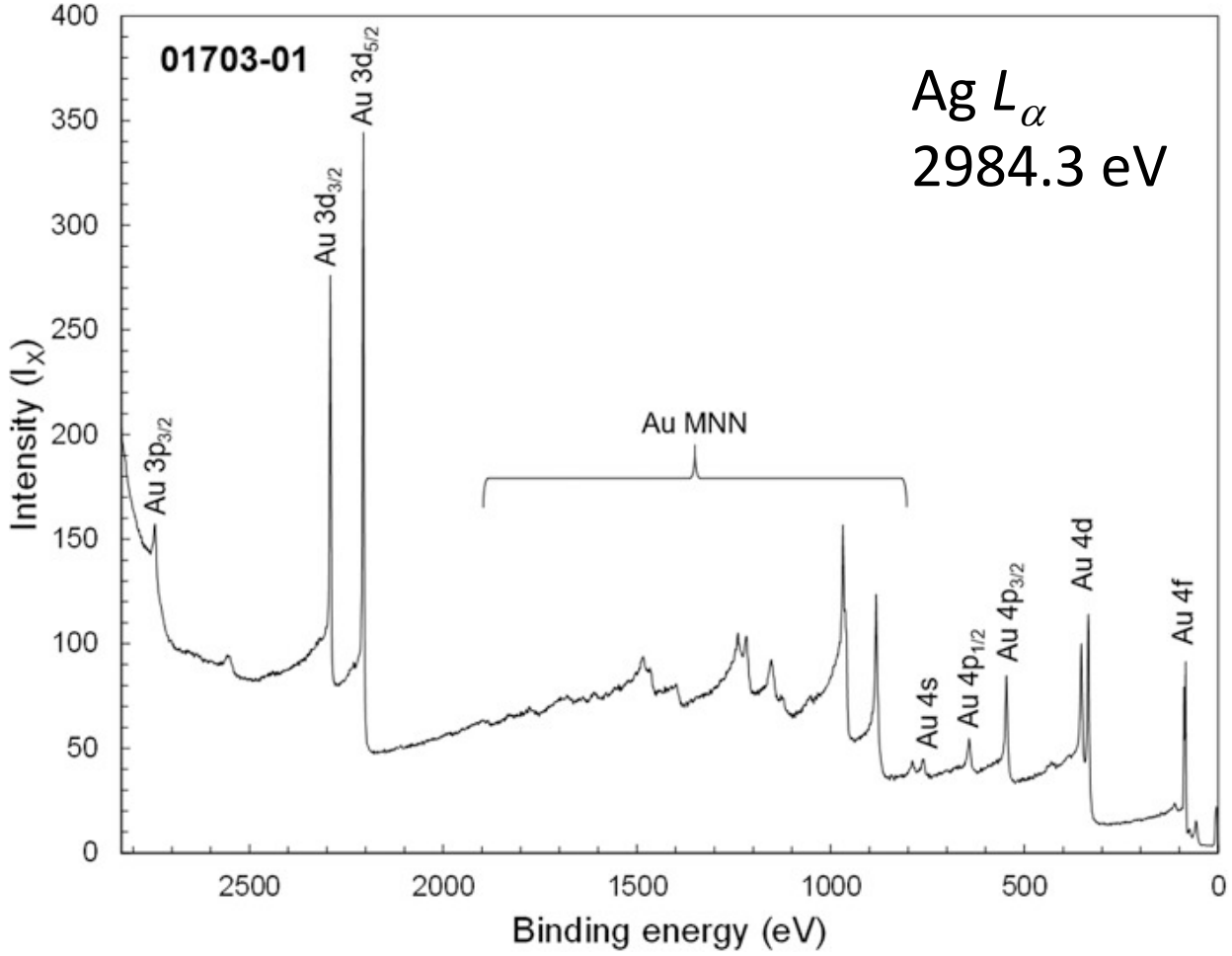

Jonathan D. P. Counsell; Alex G. Shard; David J. Cant; Christopher J. Blomfield; Parnia Navabpour; Xiaoling Zhang; *Surface Science Spectra* **28,** 024005 (2021). DOI: 10.1116/6.0001389
Copyright © 2021 Author(s)

Elemental Shifts – Higher Energy X-ray Sources

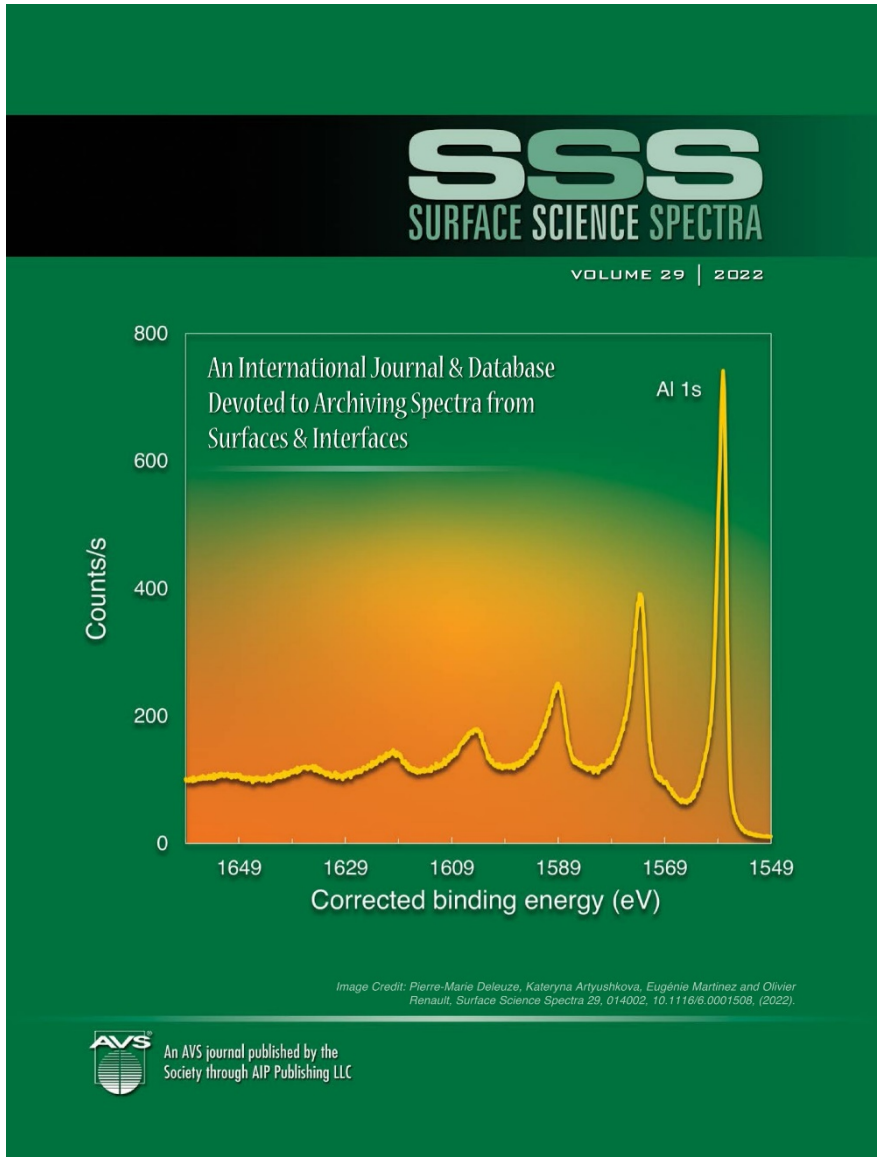

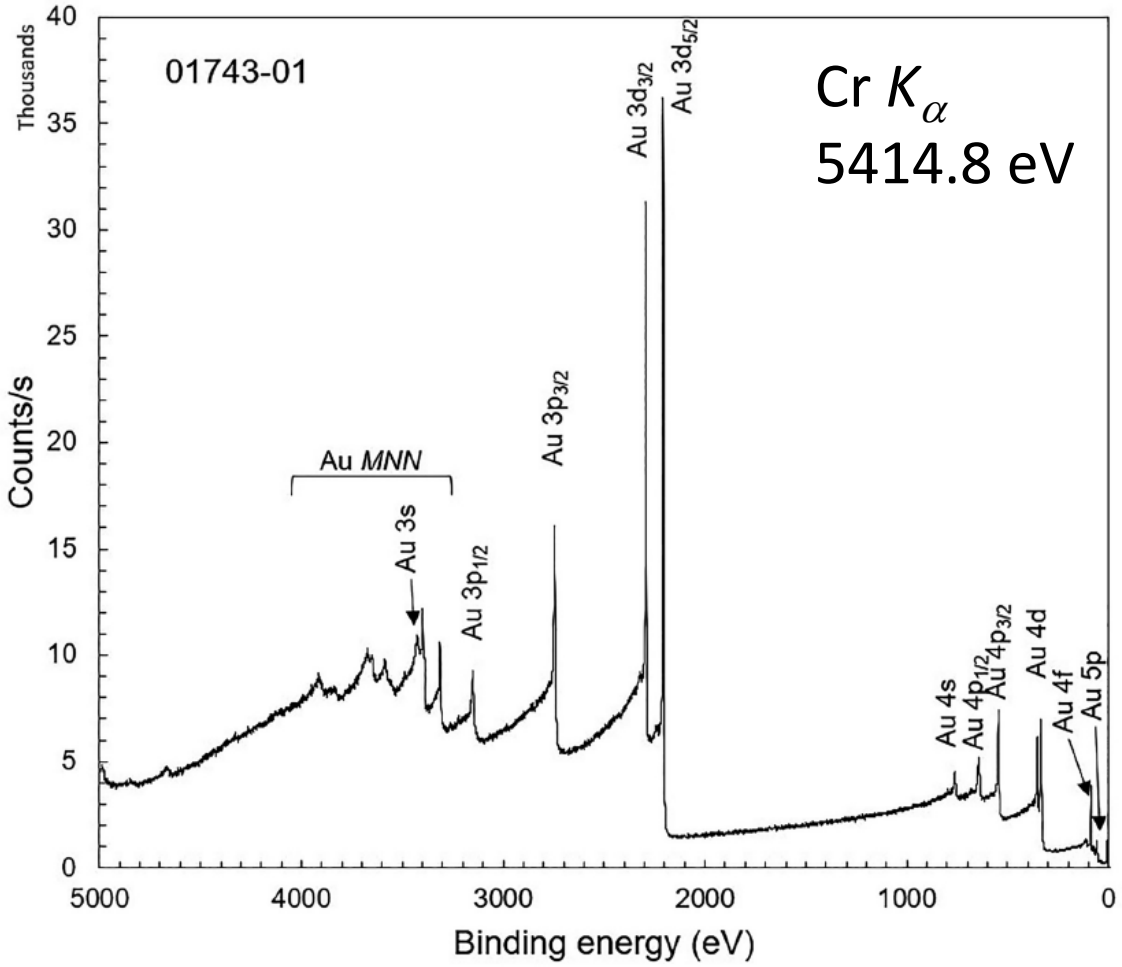

I. Hoflijk, A. Vanleenhove, I. Vaesen, C. Zborowski, K. Artyushkova, T. Conard; High energy x-ray photoelectron spectroscopy spectra of Si_3N_4 measured by Cr Kα. *Surface Science Spectra* 1 June 2022; 29 (1): 014013. https://doi.org/10.1116/6.0001524

Elemental Shifts – Higher Energy X-ray Sources

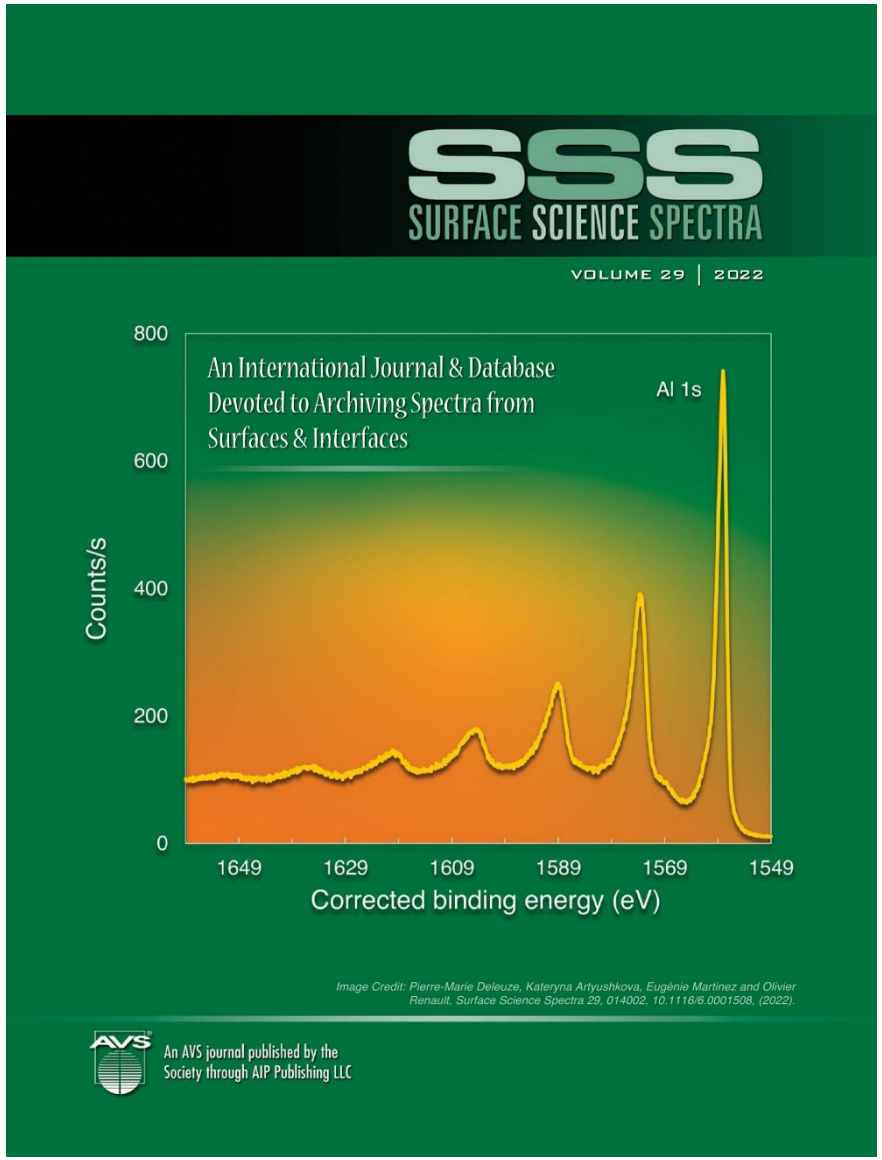

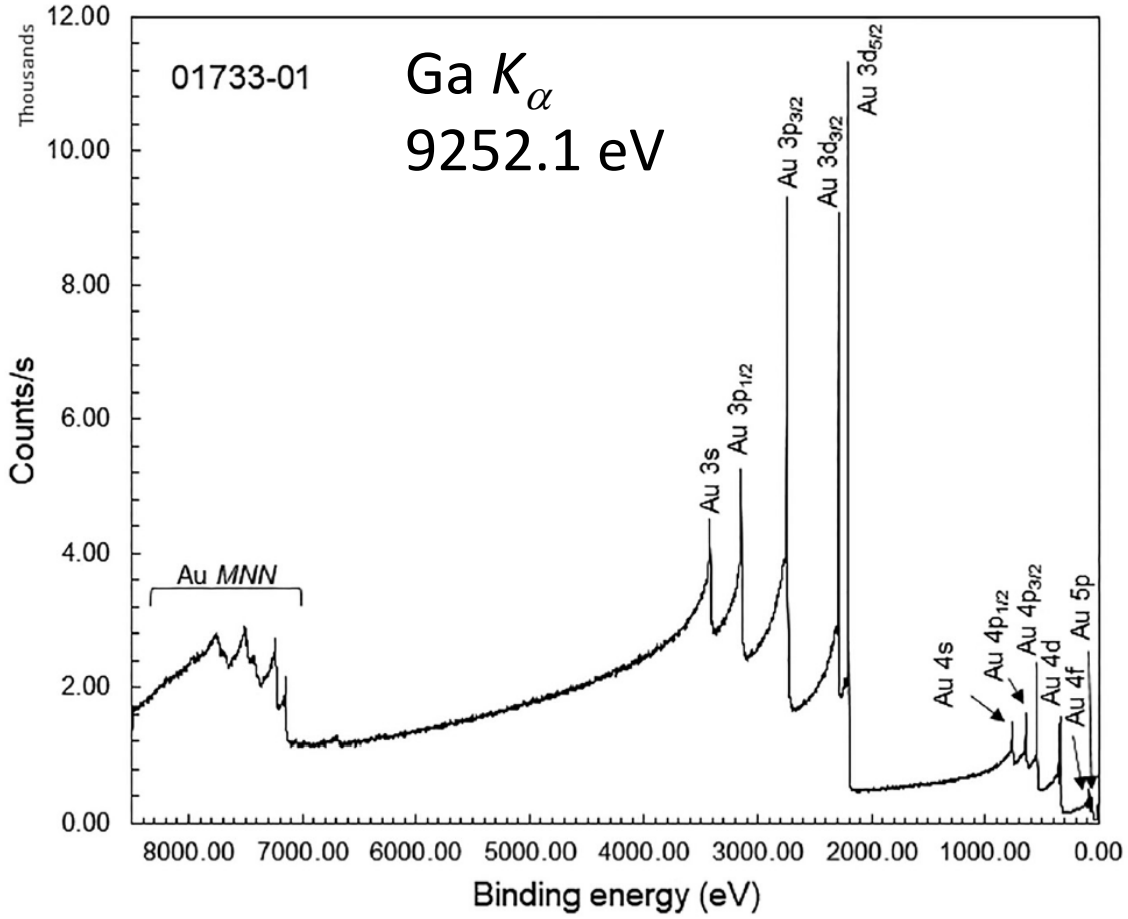

Anja Vanleenhove, Fiona Crystal Mascarenhas, Ilse Hoflijk, Inge Vaesen, Charlotte Zborowski, Thierry Conard; HAXPES on SiO_2 with Ga Kα photons. *Surface Science Spectra* 1 June 2022; 29 (1): 014012. https://doi.org/10.1116/6.0001523

Elemental Shifts

First-Row Transition Metals

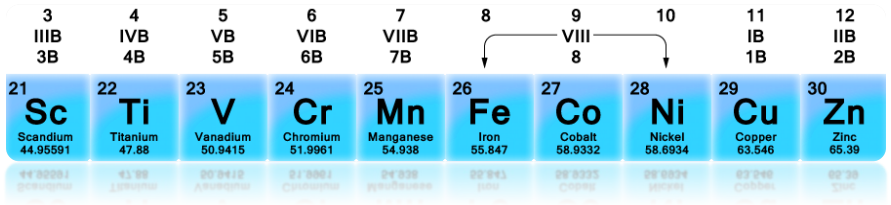

Element	Binding Energy (eV)		
	$2p_{3/2}$	3p	Δ
Sc	399	29	370
Ti	454	33	421
V	512	37	475
Cr	574	43	531
Mn	639	48	591
Fe	707	53	654
Co	778	60	718
Ni	853	67	786
Cu	933	75	858
Zn	1022	89	933

Elemental Shifts: Transition Metal Nitrides

First-Row Transition Metal Nitrides: ScN, TiN, VN, and CrN

Auger transition kinetic energies increase (binding energies decrease)

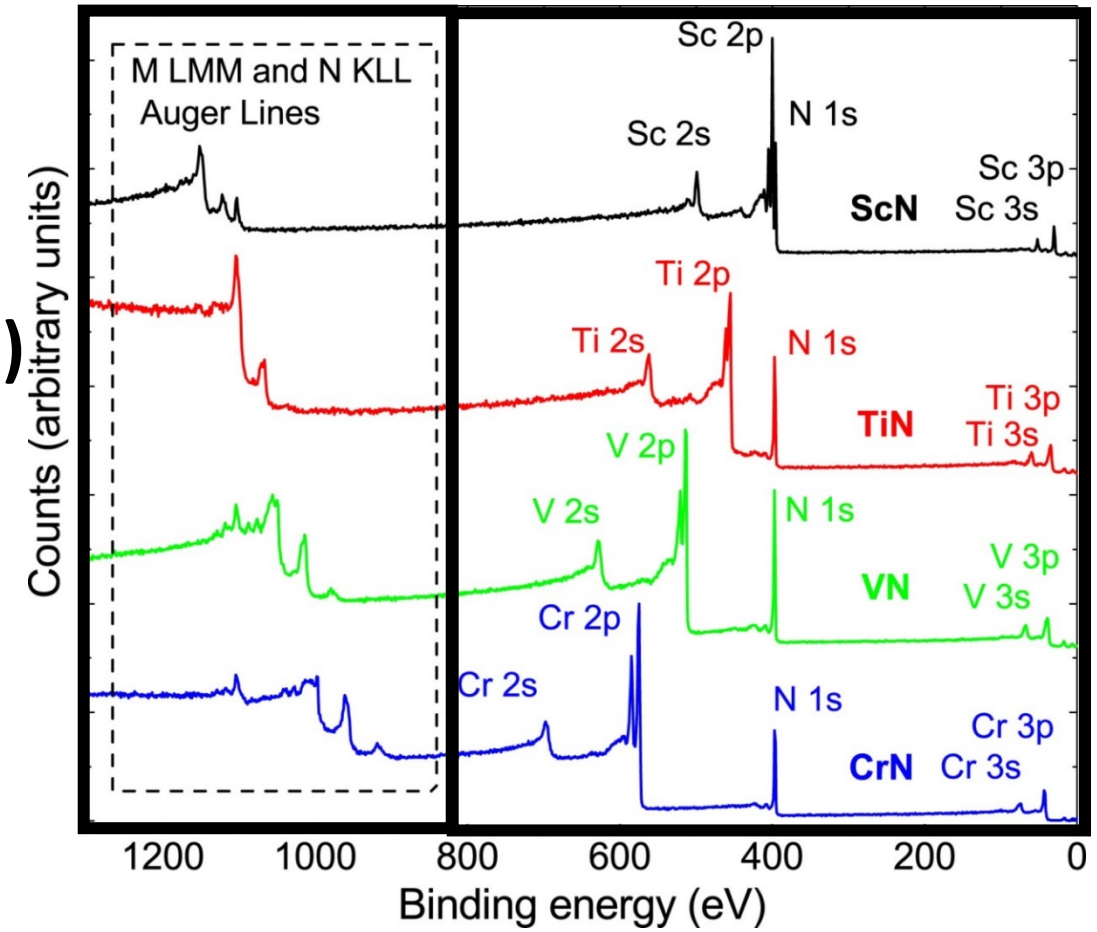

XPS Core-level binding energies increase

R. T. Haasch, T.-Y. Lee, D. Gall, C.-S. Shin, J. E. Greene, I. Petrov, *Surf. Sci. Spectra*, **7**, 169 (2000), *Surf. Sci. Spectra*, **7**, 193 (2000), *Surf. Sci. Spectra*, **7**, 221 (2000), *Surf. Sci. Spectra*, **7**, 250 (2000).

Spin-orbit Splitting

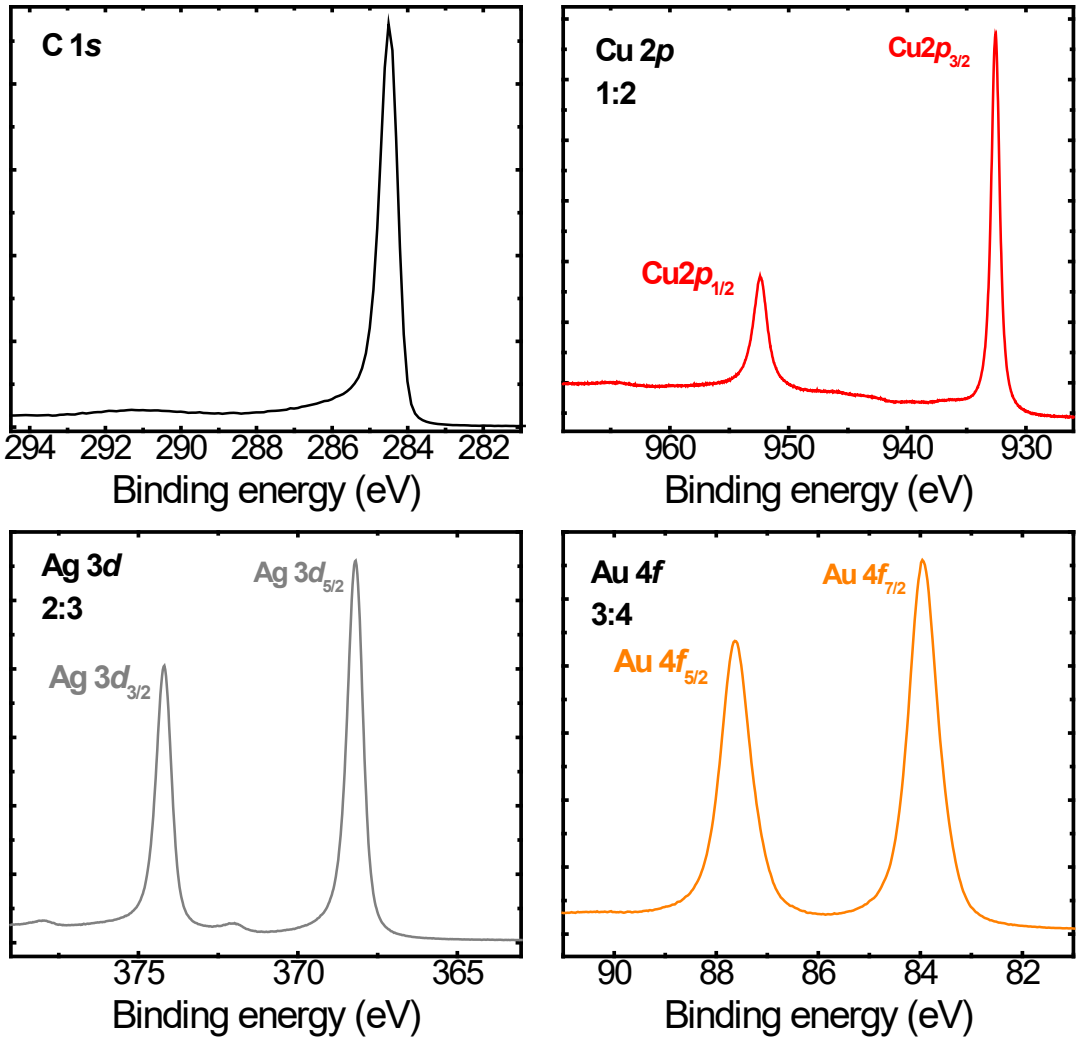

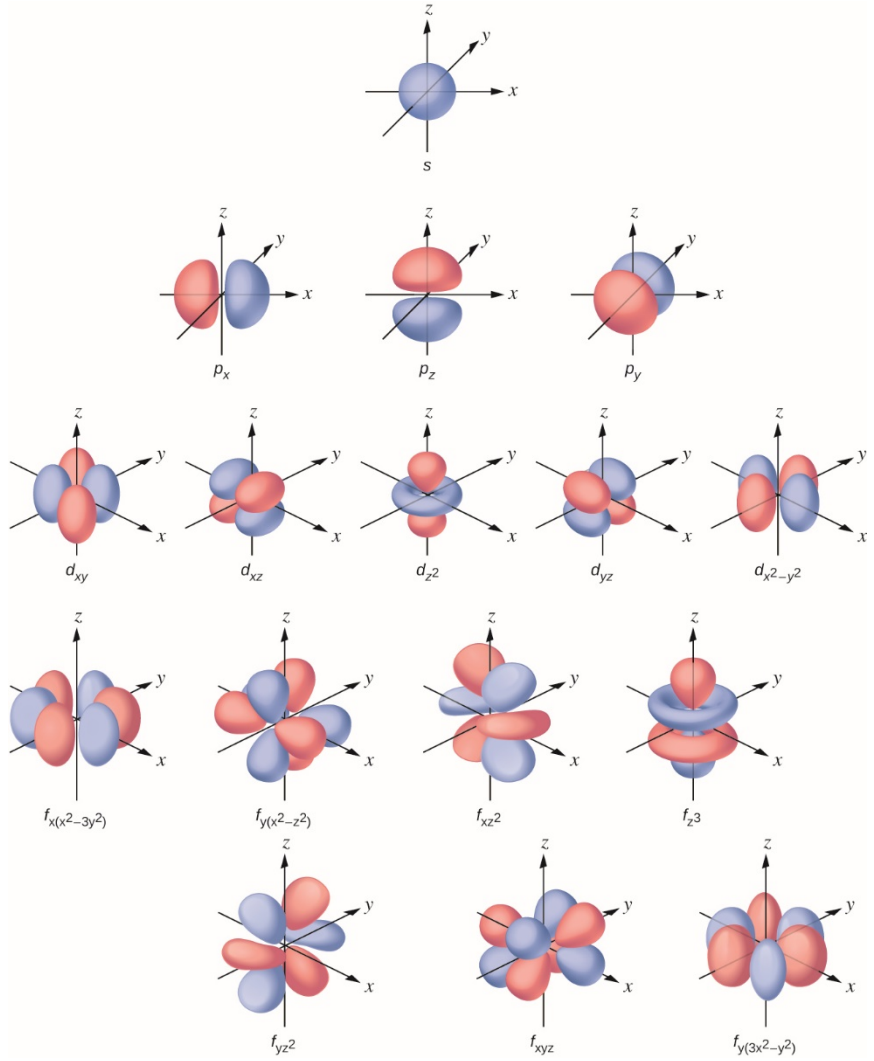

R. T. Haasch, "X-ray Photoelectron Spectroscopy (XPS) and Auger Electron Spectroscopy (AES)," in *Practical Materials Characterization*, M. Sardela, ed., (Springer Science + Business Media, New York, 2014). ISBN 978-1-4614-9280-1. doi: 10.1007/978-1-4614-9281-8_3.

Atomic Orbitals and Quantum Numbers. (2019, June 5). https://chem.libretexts.org/@go/page/122444

Spin-orbit Splitting

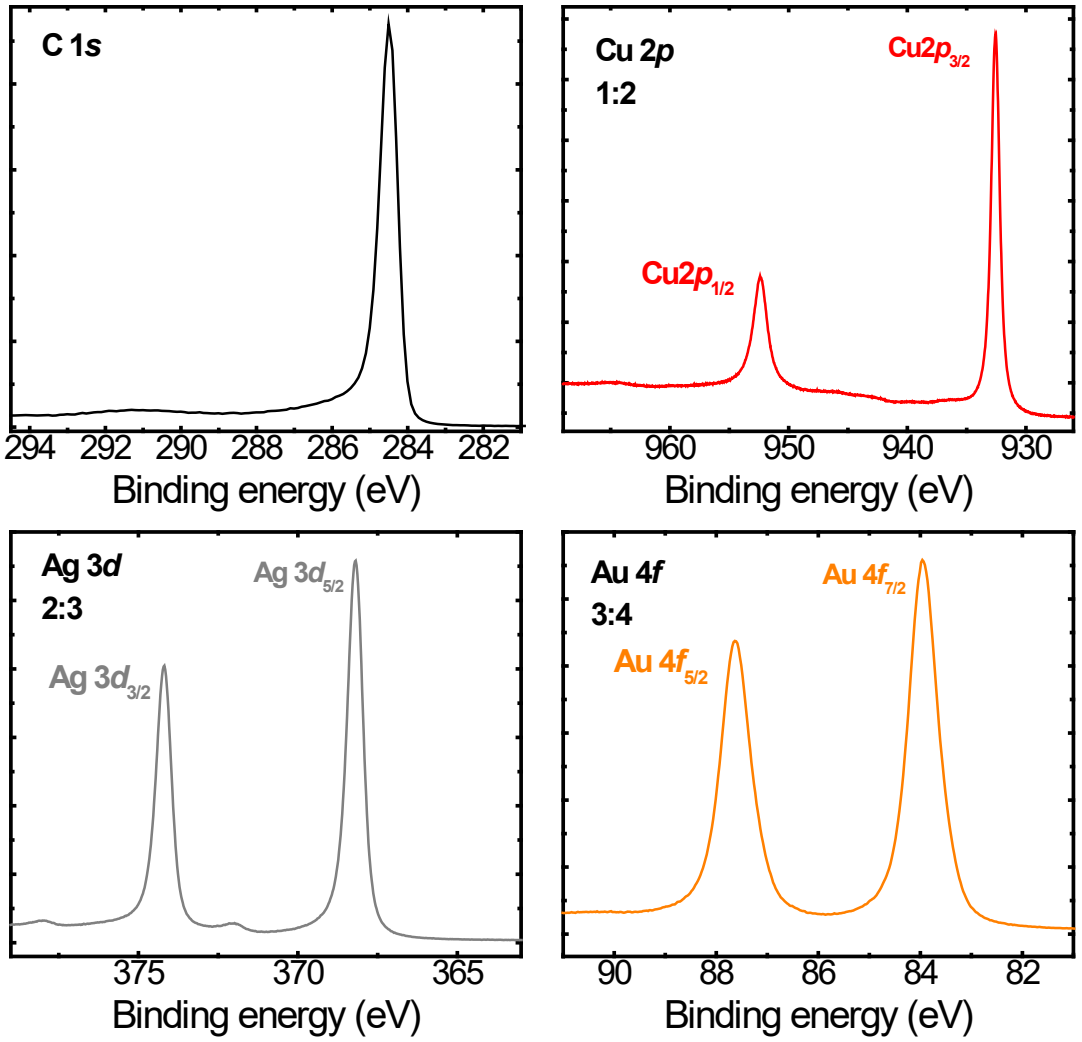

Electron spin: $s = \pm ½$

Orbital angular momentum:
l = 0, 1, 2, 3 … for *s, p, d, f* orbitals

$$j = |l \pm s|$$

Momentum quantum number:
m_j, $-j$ to j ($2j + 1$ states)

R. T. Haasch, "X-ray Photoelectron Spectroscopy (XPS) and Auger Electron Spectroscopy (AES)," in *Practical Materials Characterization*, M. Sardela, ed., (Springer Science + Business Media, New York, 2014). ISBN 978-1-4614-9280-1. doi: 10.1007/978-1-4614-9281-8_3.
Atomic Orbitals and Quantum Numbers. (2019, June 5). https://chem.libretexts.org/@go/page/122444

Graphene Transfer

A sustainable approach to large area transfer of graphene

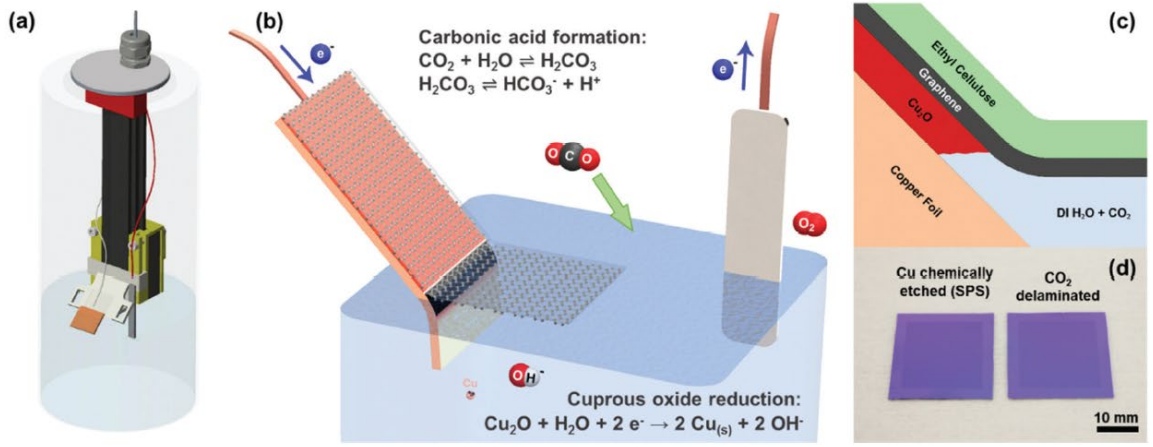

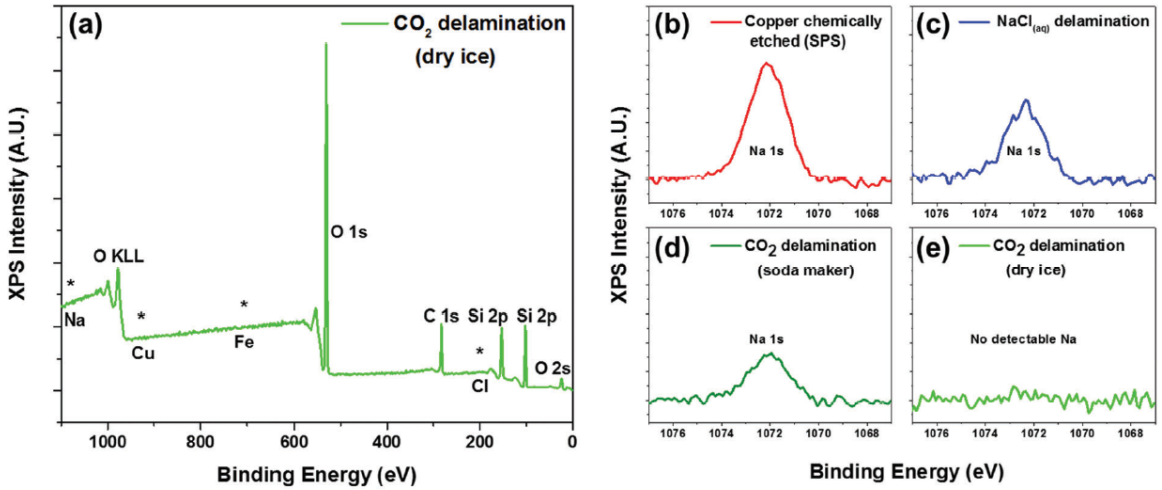

a) XPS survey of CO_2 delamination (from dry ice)
b) Chemically etched (sodium persulphate)
c) NaCl electrolyte delaminated
d) CO_2 delamination using compressed CO_2 from soda maker
e) Delamination using carbonic acid generated from dry ice pellets

M. C. Wang, W. Moestopo, S. Takekuma, S. Farabi, R. T. Haasch, S.-W. Nam, "Sustainable approach for large area transfer of graphene and recycle of the catalyst substrate," *J. Mater. Chem. C*, **5**, 11226 (2017). doi:10.1039/c7tc02487h.

Chemical Shifts

Electronegativity Effects

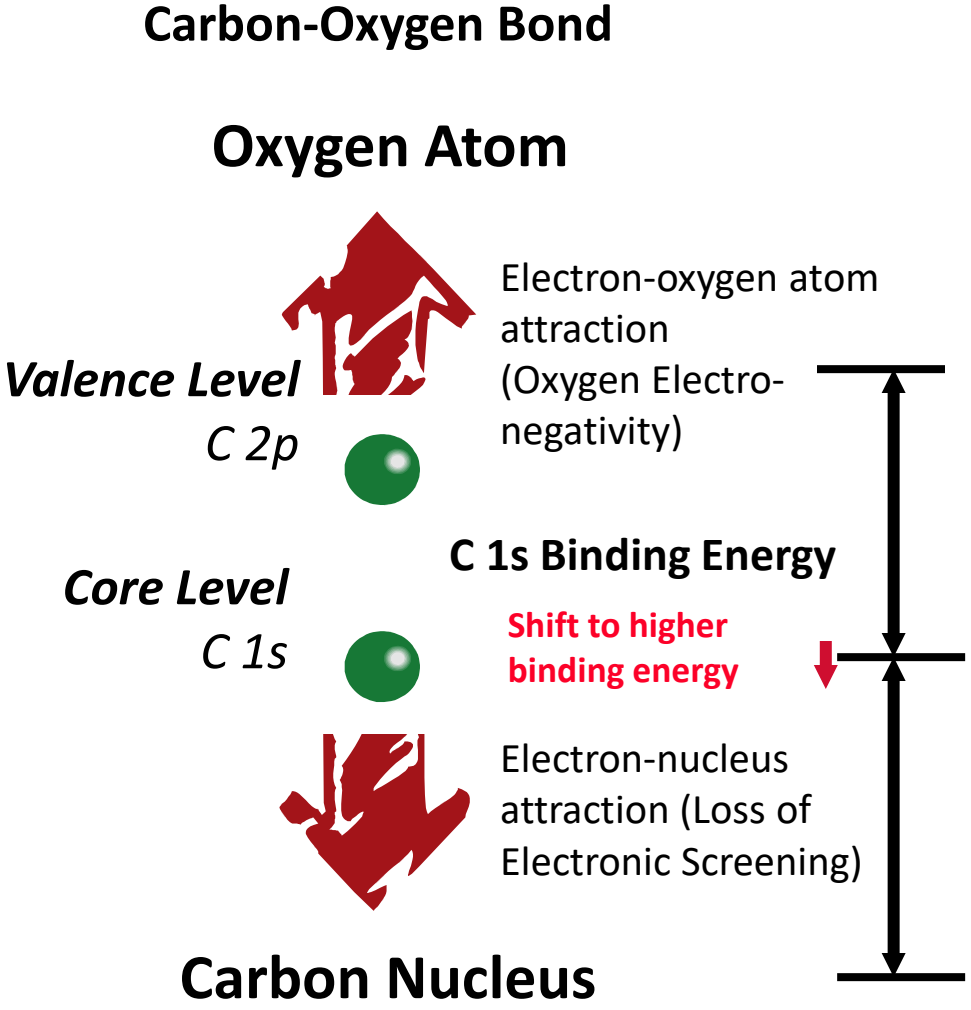

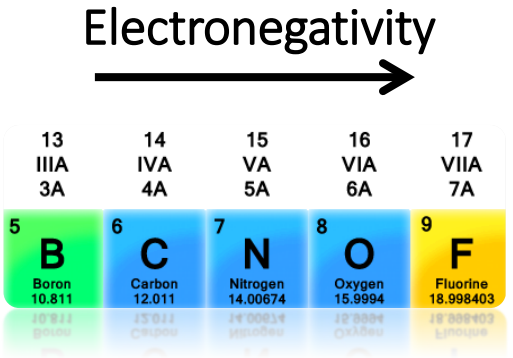

Functional Group		C 1s Binding Energy
hydrocarbon	C-H, C-C	285.0
amine	C-N	286.0
alcohol, ether	C-O-H, C-O-C	286.5
Cl bound to C	C-Cl	286.5
F bound to C	C-F	287.8
carbonyl	C=O	288.0

Chemical Shifts

XPS of polymethylmethacrylate

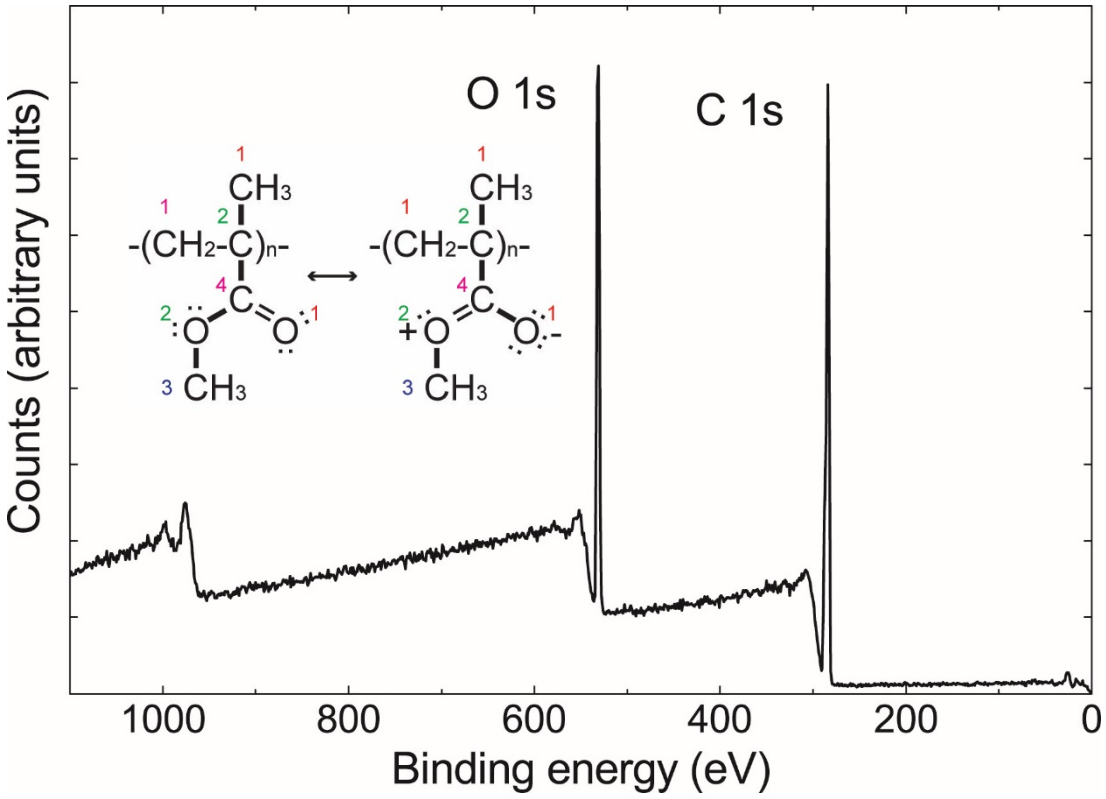

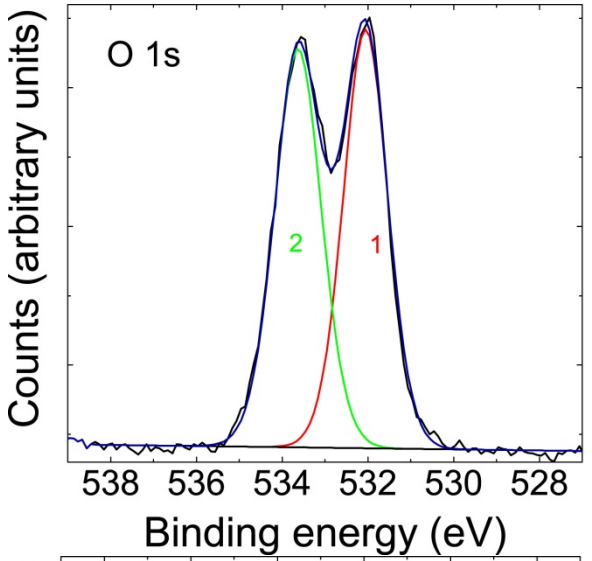

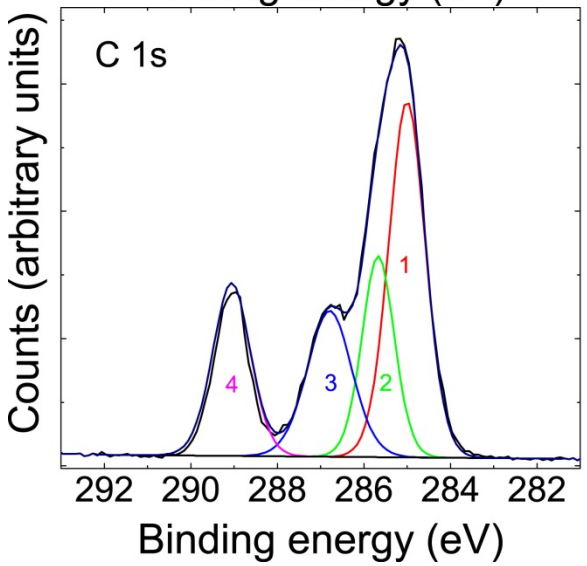

R. T. Haasch, "X-ray Photoelectron Spectroscopy (XPS) and Auger Electron Spectroscopy (AES)," in *Practical Materials Characterization*, M. Sardela, ed., (Springer Science + Business Media, New York, 2014). ISBN 978-1-4614-9280-1. doi: 10.1007/978-1-4614-9281-8_3.

Superhydrophobic Materials

Superhydrophobic Surfaces from Naturally Derived Hydrophobic Materials

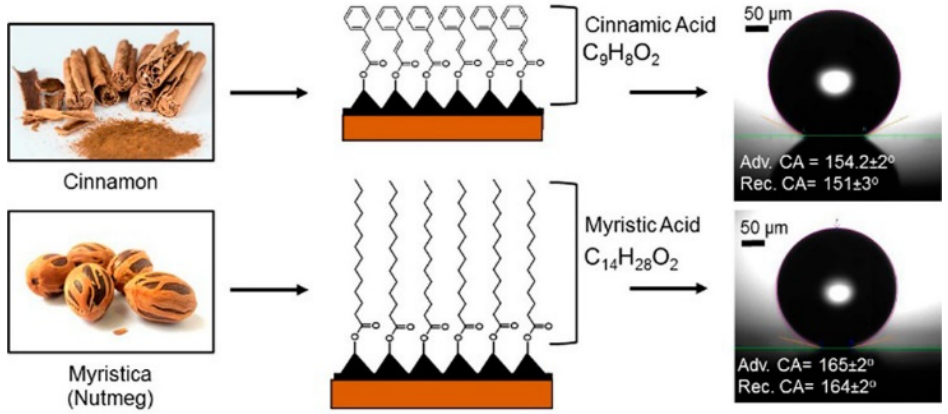

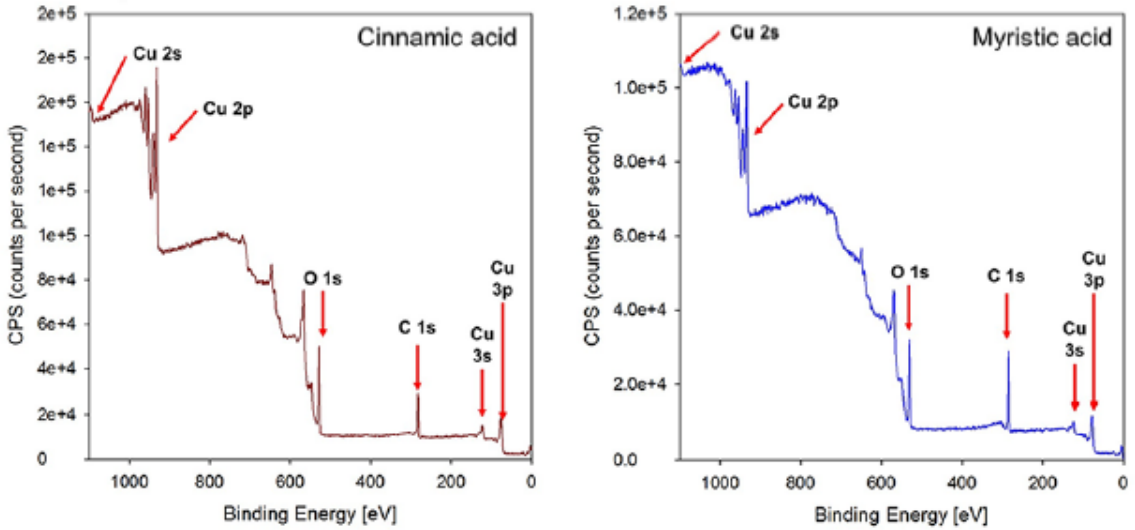

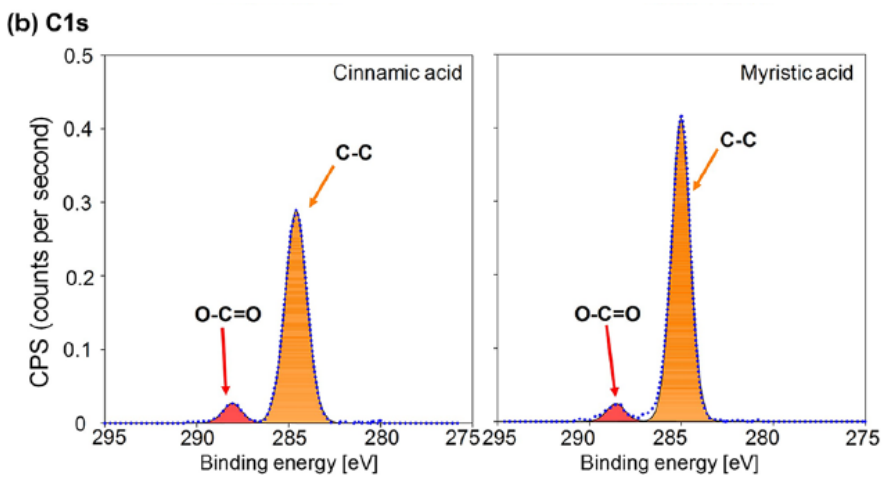

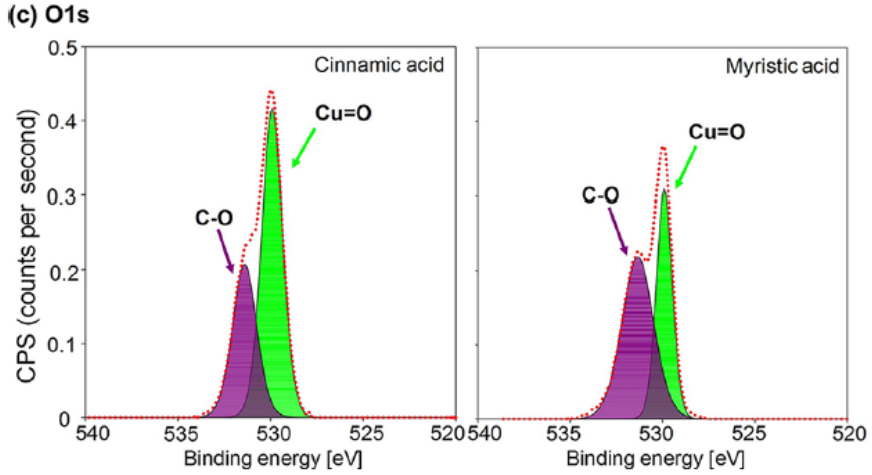

S. M. R. Razavi, J. Oh, S. Sett, L. Feng, X. Yan, M. J. Hoque, A. Liu, R. T. Haasch, M. Masoomi, R. Bagheri, N. Miljkovic, "Superhydrophobic Surfaces Made From Naturally Derived Hydrophobic Materials," *ACS Sustainable Chem. Eng.*, 5(12), 11362 (2017). doi:10.1021/acssuschemeng.7b02424.

Solid Electrolyte Interphase (SEI)

Parallel pathways for the transport and intercalation of Li ions into an active particle and the growth of the SEI layer through degradation reactions of solvent molecules with Li ions.

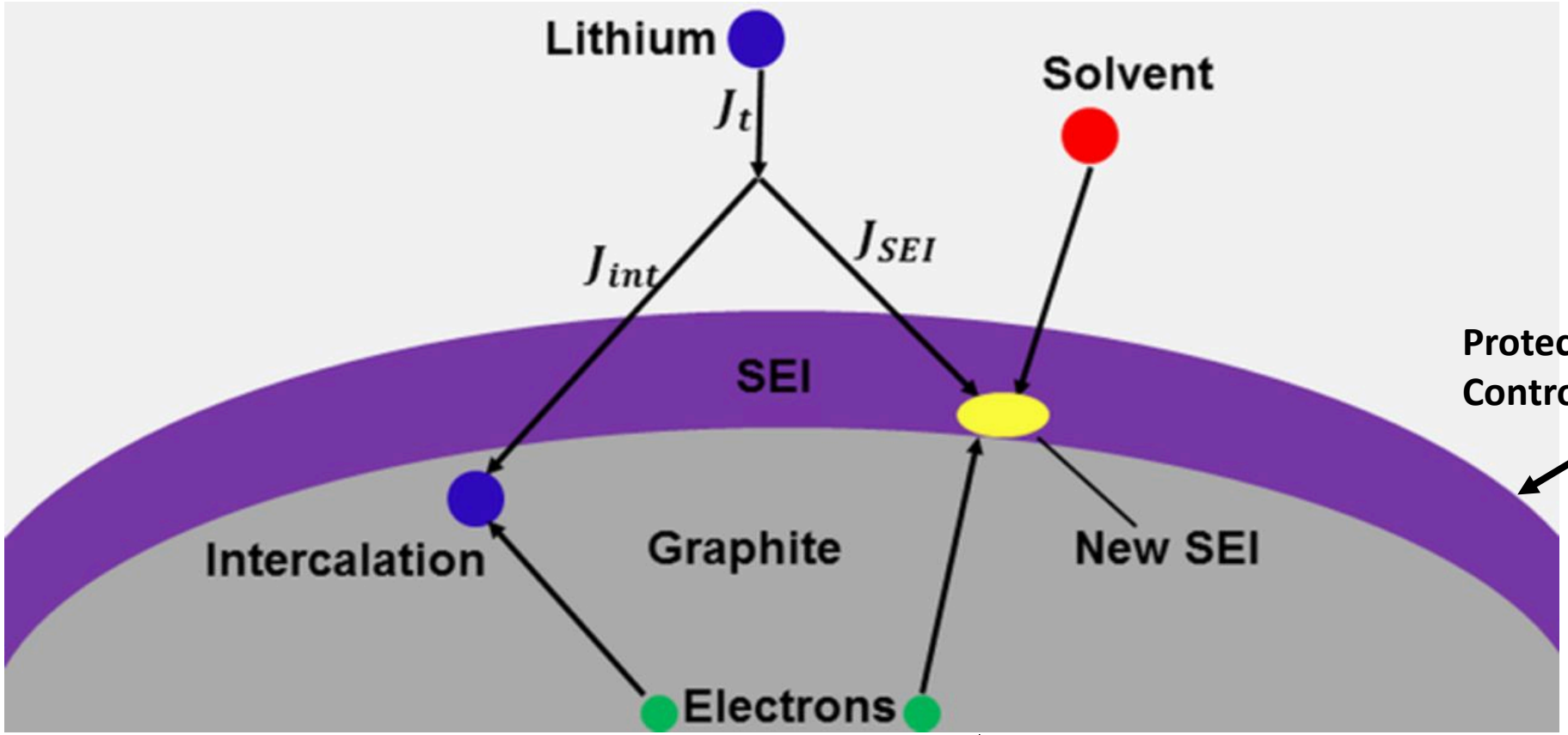

A. A. Tahmasbi et al. J. Electrochem. Soc. 2017;164:A1307-A1313

Journal of The Electrochemical Society

Cathode (positive electrode)- $LiNi_{0.8}Co_{0.2}O_2$

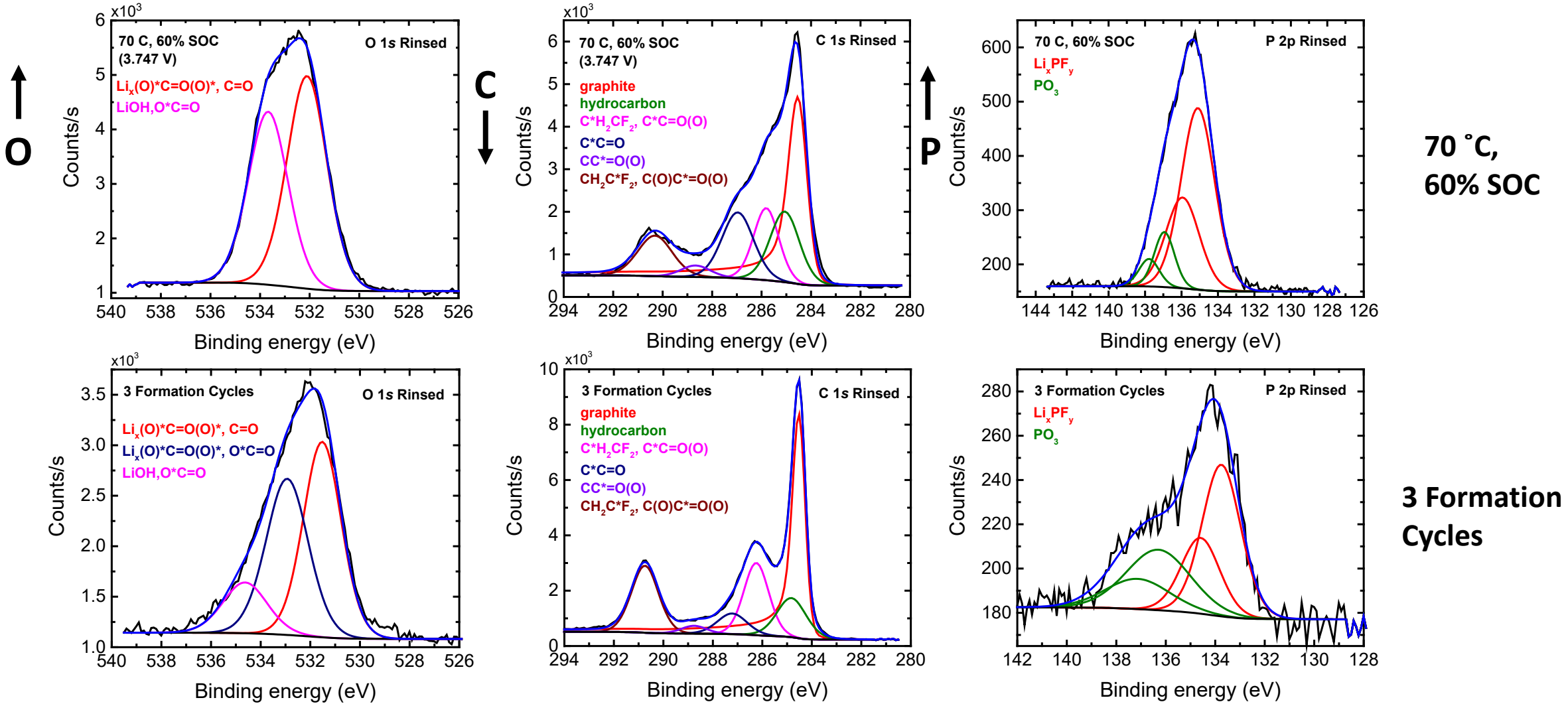

D. P. Abraham, J. Liu, C. H. Chen, Y. E. Hyung, M. Stoll, N. Elsen, S. MacLaren, R. Twesten, R. Haasch, E. Sammann I. Petrov, K. Amine, G. Henriksen, "Diagnosis of power fade mechanisms in high-power lithium-ion cells," *J. Power Sources*, **119-121**, 511-516 (2003).

R. T. Haasch, D. P. Abraham, "$LiNi_{0.8}Co_{0.2}O_2$-based high-power lithium-ion battery positive electrodes analyzed by X-ray photoelectron spectroscopy," *Surface Science Spectra*, **23**, 112-172 (2016).

Anode (negative electrode)- Si Based Materials

Si powders and electrodes for high-energy lithium-ion cells

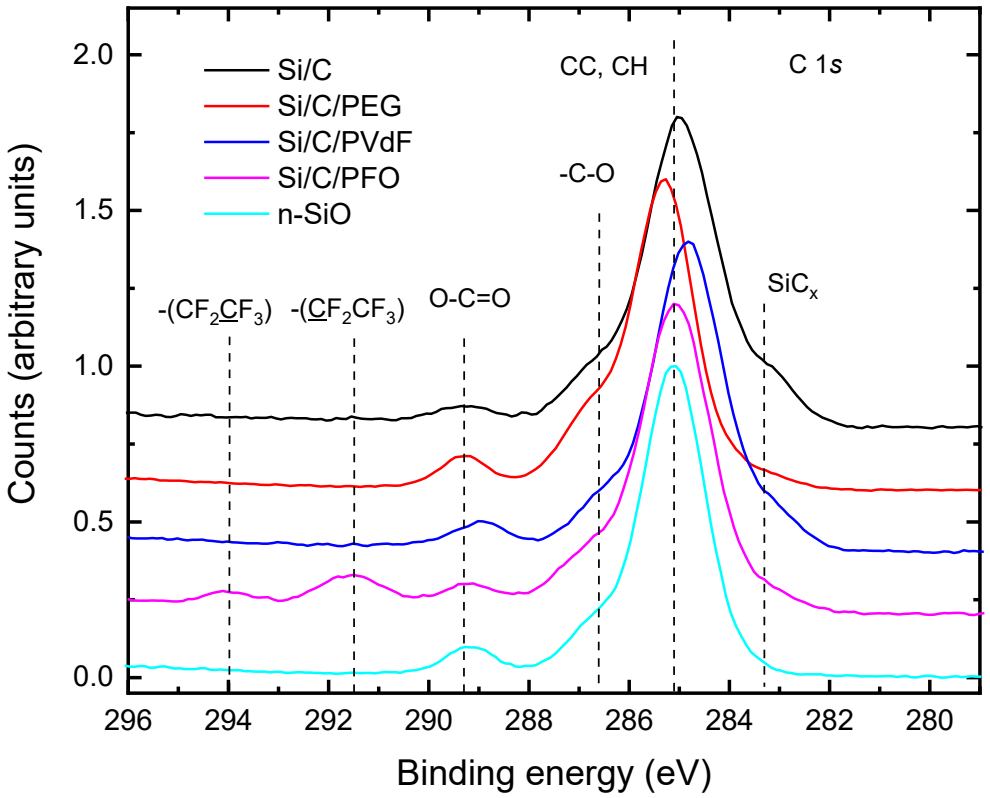

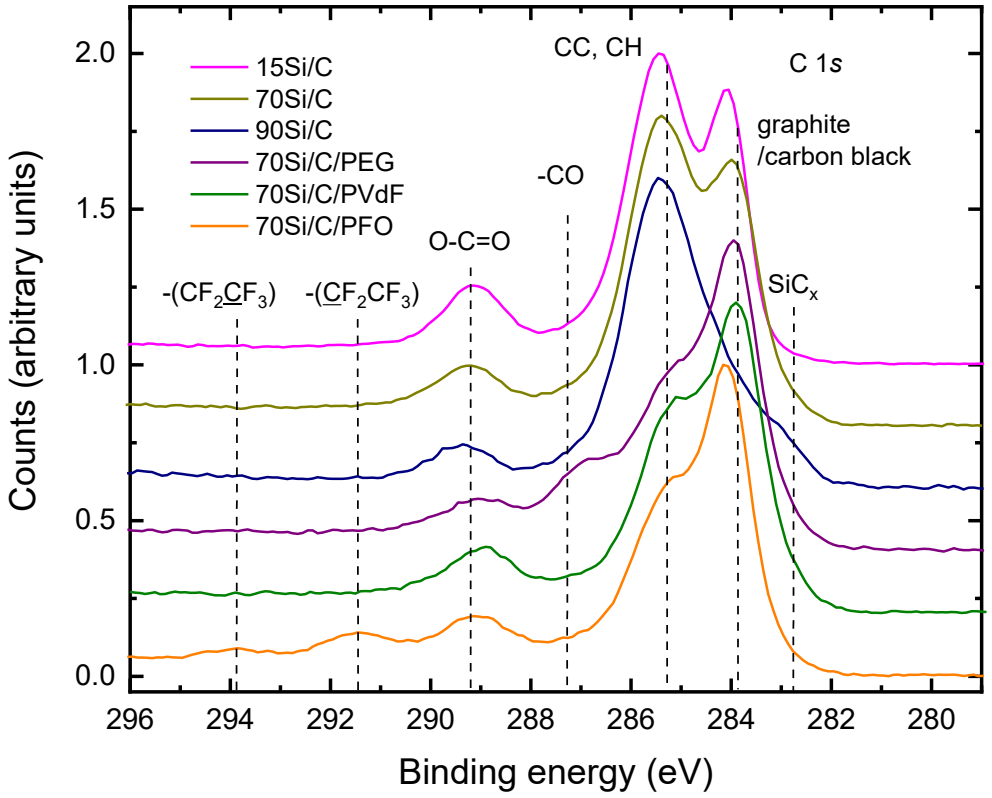

R. T. Haasch, D. P. Abraham, "Si powders and electrodes for high-energy lithium-ion cells," *Surf. Sci. Spectra*, **26**, 016801 (2020). doi:10.1116/1.5130764.

Dissolvable Metals

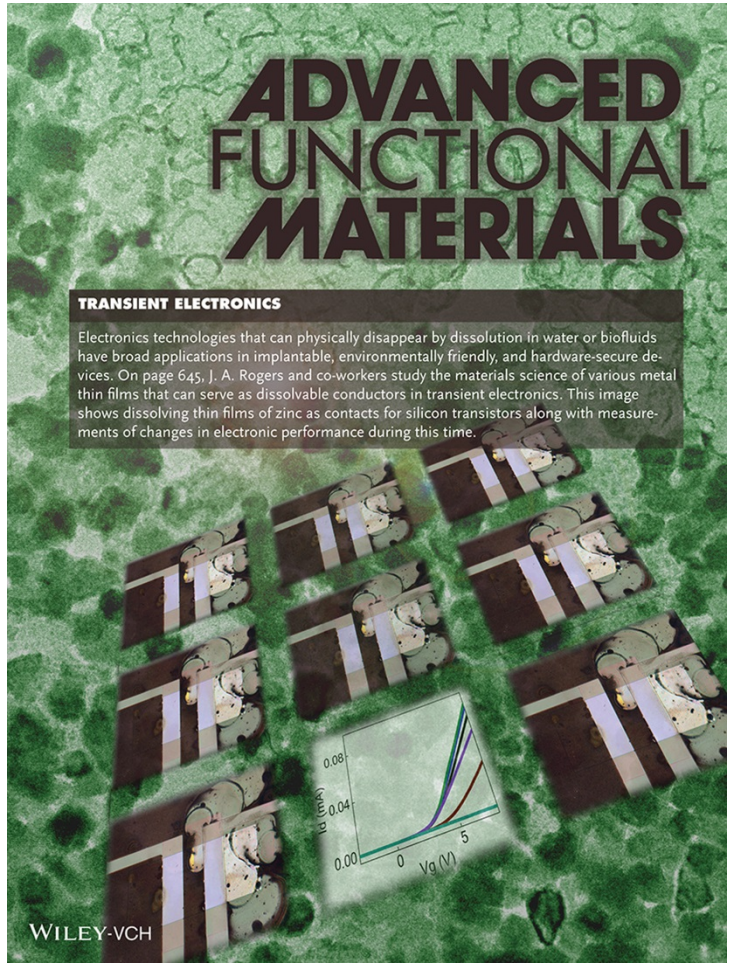

Materials Views
www.MaterialsViews.com
ADVANCED FUNCTIONAL MATERIALS
www.afm-journal.de

Dissolvable Metals for Transient Electronics

*Lan Yin, Huanyu Cheng, Shimin Mao, Richard Haasch, Yuhao Liu, Xu Xie, Suk-Won Hwang, Harshvardhan Jain, Seung-Kyun Kang, Yewang Su, Rui Li, Yonggang Huang, and John A. Rogers**

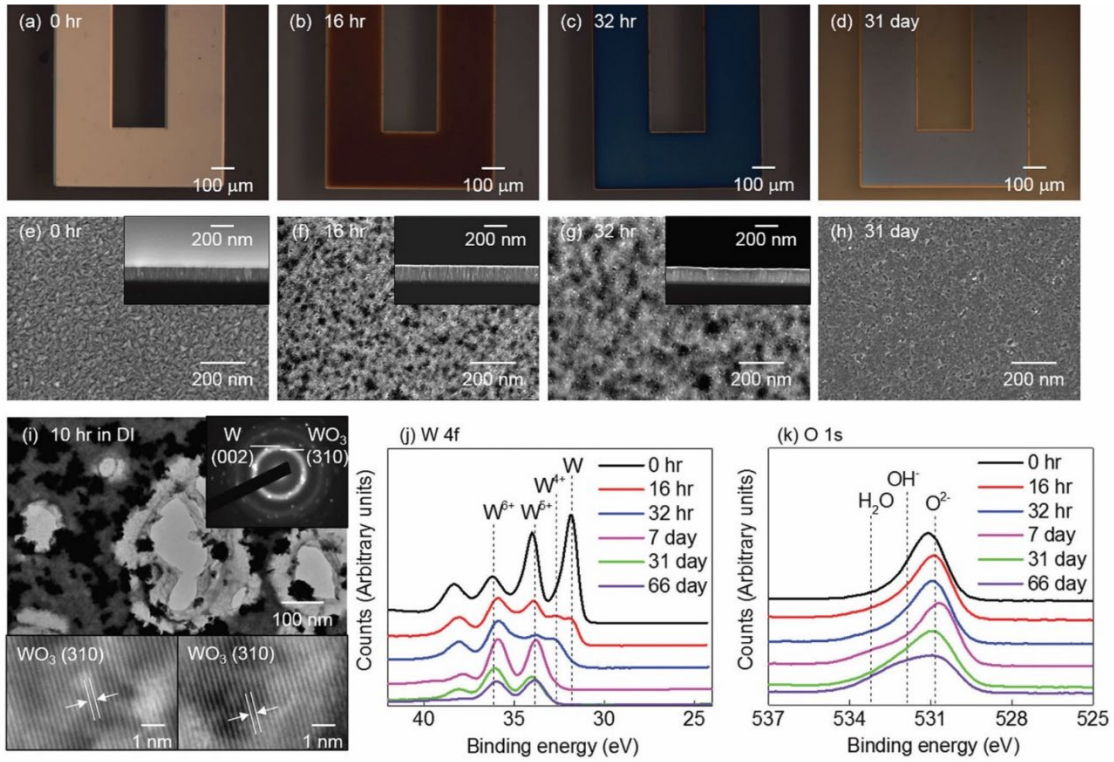

L. Yin, H. Cheng, S. Mao, R. Haasch, Y. Liu, X. Xie, S.-W. Hwang, H. Jain, S.-K. Kang, Y. Su, R. Li, Y. Huang, J. A. Rogers, "Dissolvable Metals for Transient Electronics," *Adv. Funct. Mater.*, **24**, 645 (2014).

Transition Metal Nitrides

N 1s spectra of First-Row Transition Metal Nitrides: ScN, TiN, VN, and CrN

p-d hybridization 8 MO's

	Anti-bonding e^- /Formula Unit (nominal)	Binding Energy, eV
ScN	-0.17 (0)	396.1
TiN	1 (1)	397.3
VN	1.9 (2)	397.0
CrN	2.9 (3)	396.7

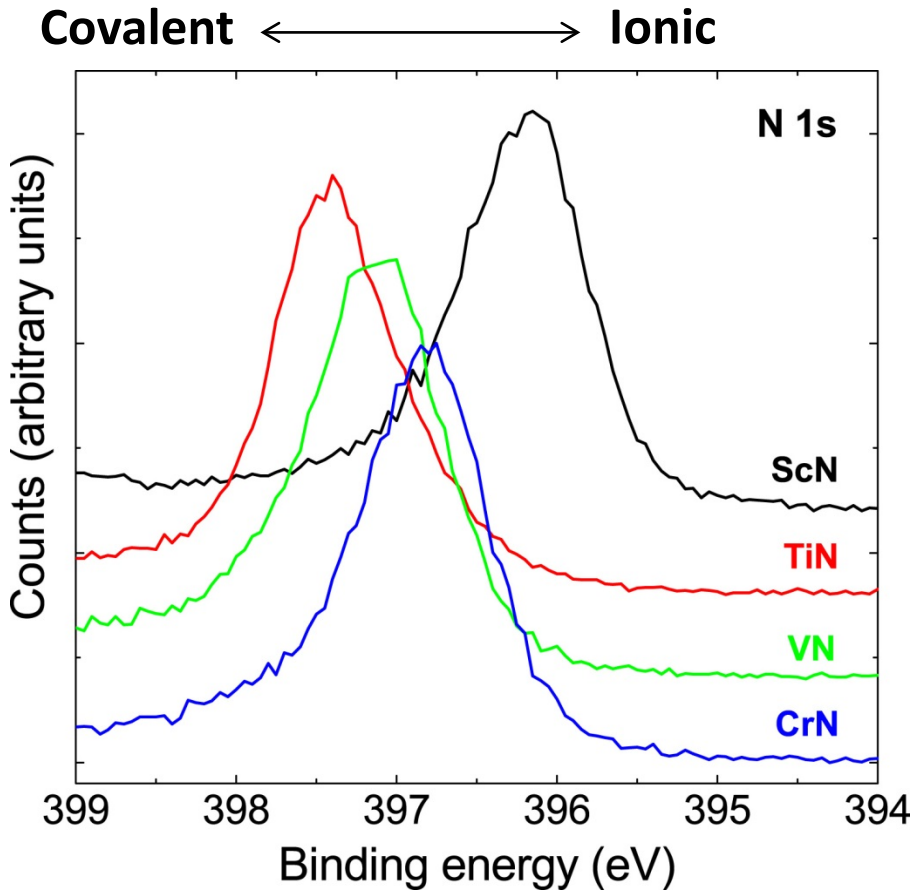

R. T. Haasch, T.-Y. Lee, D. Gall, C.-S. Shin, J. E. Greene, I. Petrov, *Surf. Sci. Spectra*, **7**, 169 (2000), *Surf. Sci. Spectra*, **7**, 193 (2000), *Surf. Sci. Spectra*, **7**, 221 (2000), *Surf. Sci. Spectra*, **7**, 250 (2000).

Quantitative Surface Analysis: XPS

detector count rate A_i

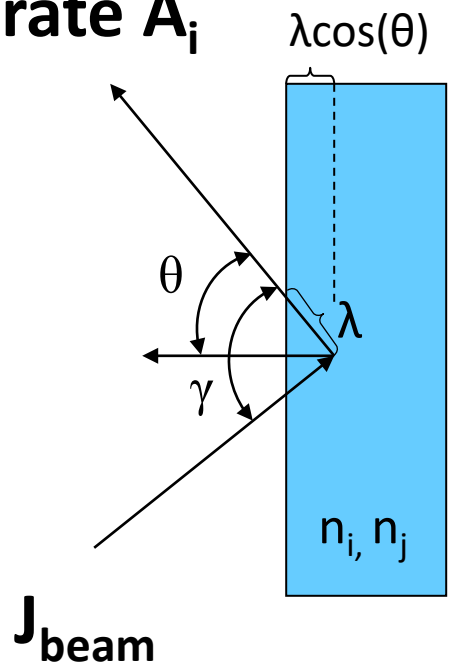

Assuming a Homogeneous sample:

A_i = detector count rate

A_i = (electrons/volume)(volume)

A_i = ($N_i\sigma_i(\gamma)JT(E_i)$)($a\lambda_i(E_i)\cos\theta$)

Sample Dependent Terms

where: N = atoms/cm^3

$\sigma(\gamma)$ = photoelectric (scattering) cross-section, cm^2

$\lambda(E_i)$ = inelastic electron mean-free path, cm

Instrument Dependent Terms

J = X-ray flux, photon/cm^2-sec

$T(E_i)$ = analyzer transmission function

a = analysis area, cm^2

θ = photoelectron emission angle

Quantitative Surface Analysis: XPS

By assuming the concentration to be a relative ratio of atoms, we can neglect the terms that depend only on the instrument:

$$N_i = A_i/\sigma_i T(E_i)\lambda_i(E_i)$$

It is difficult to accurately determine λ_i so it is usually neglected. Modern acquisition and analysis software can account for the transmission function.

$$N_i = A_i / S_i$$

$$\mathbf{C_i = A_i/S_i \,/\, \Sigma\, A_{i,j}/S_{i,j}}$$

The values of S are determined theoretically or empirically with standards.

XPS is considered to be a *semi*-quantitative technique.

Quantitative Surface Analysis: XPS

XPS Relative Elemental Sensitivities

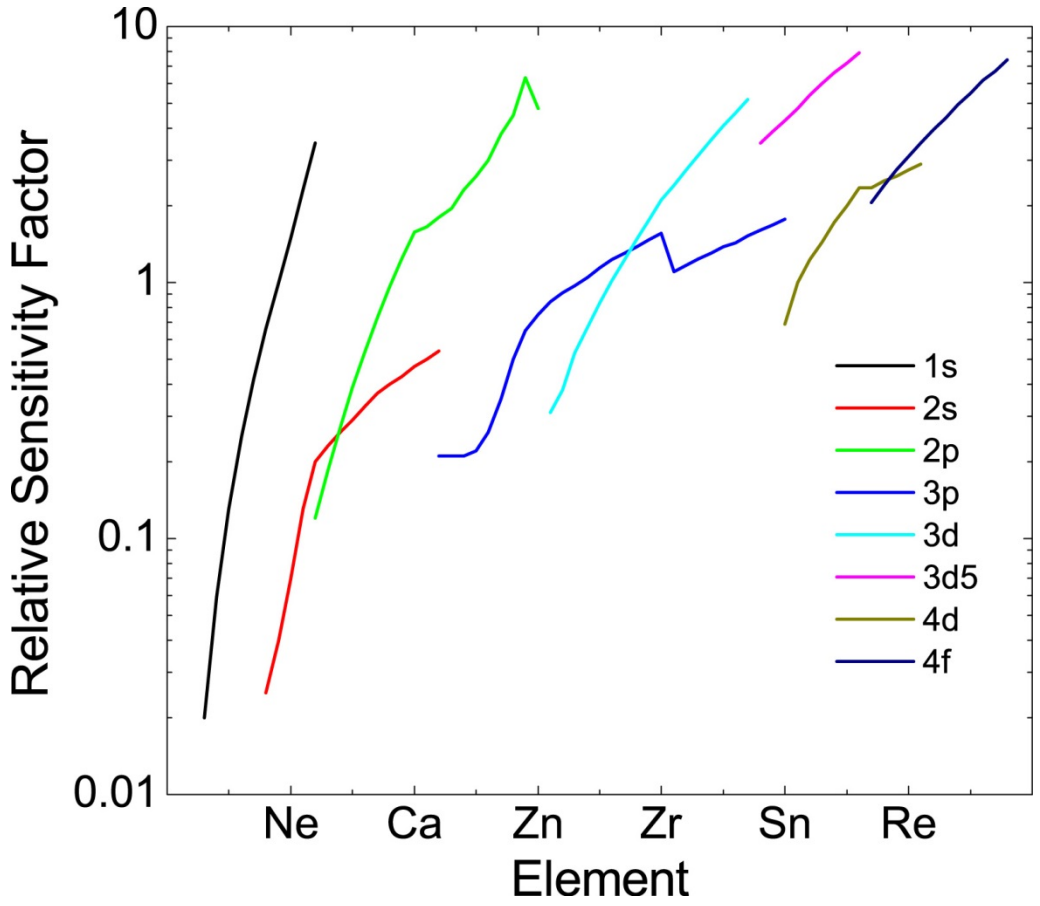

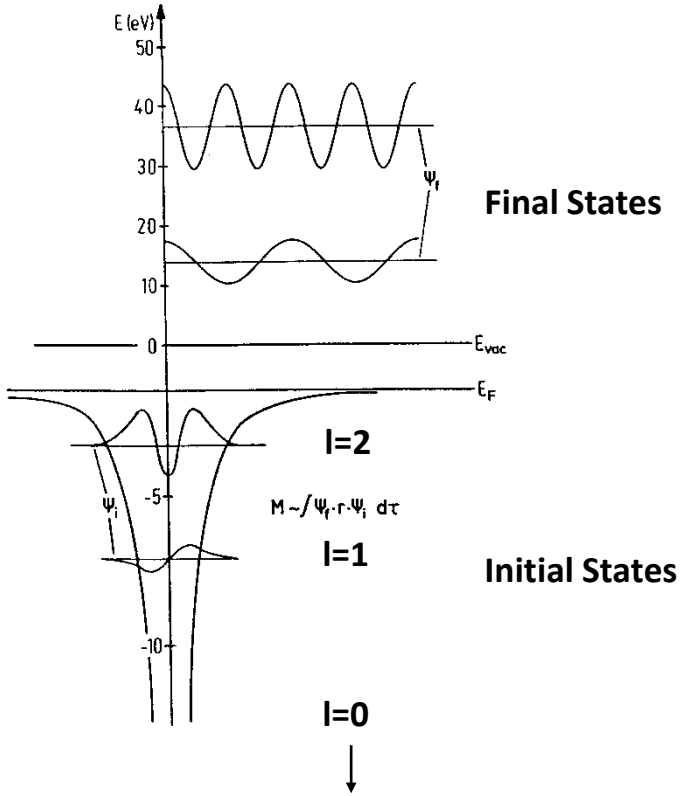

S. Hüfner, *Photoelectron Spectroscopy Principles and Applications*, Second Edition, (Springer, Berlin Heidelberg, 1996). ISBN 3-540-60875-3.

NCM Family of Oxide Materials - Raw Powder

Lithium-bearing Oxides for Rechargeable Li-ion Batteries: NCM_{xyz} ($LiNi_{x/10}Co_{y/10}Mn_{z/10}O_2$, with x+y+z=10)

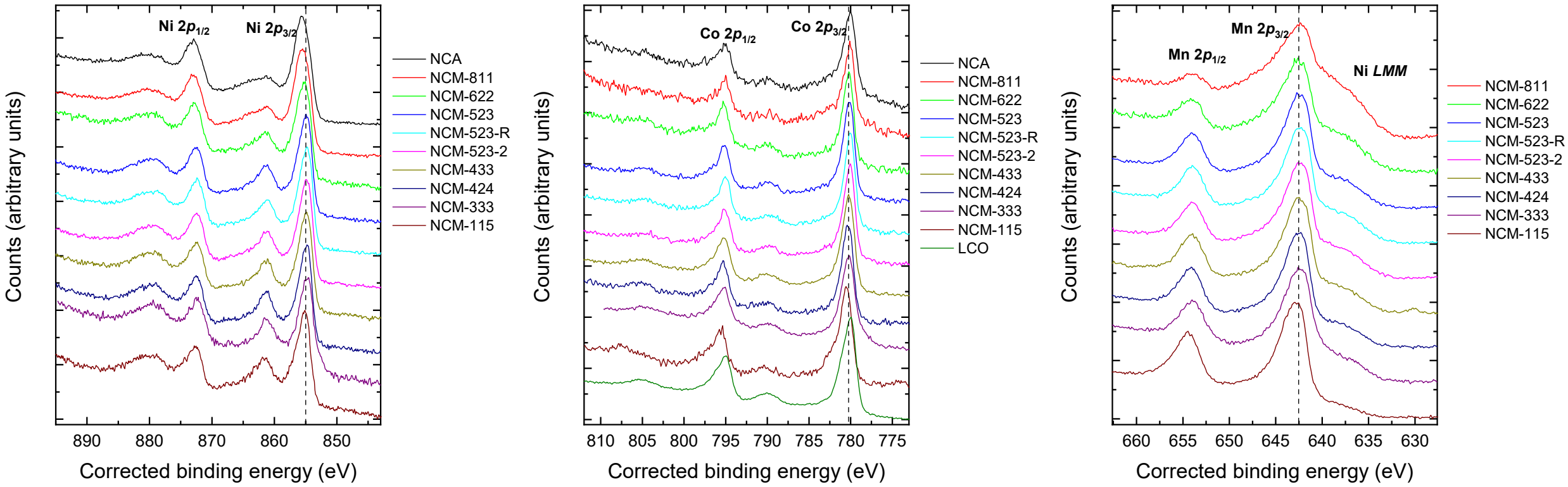

R. T. Haasch, S. E. Trask, D. P. Abraham, "Lithium-bearing oxides for rechargeable Li-ion batteries," *Surf. Sci. Spectra*, **26**, 014002 (2019). doi:10.1116/1.5080232.

NCM Family of Oxide Materials - Raw Powder

Lithium-bearing Oxides for Rechargeable Li-ion Batteries: NCM_{xyz} ($LiNi_{x/10}Co_{y/10}Mn_{z/10}O_2$, with x+y+z=10)

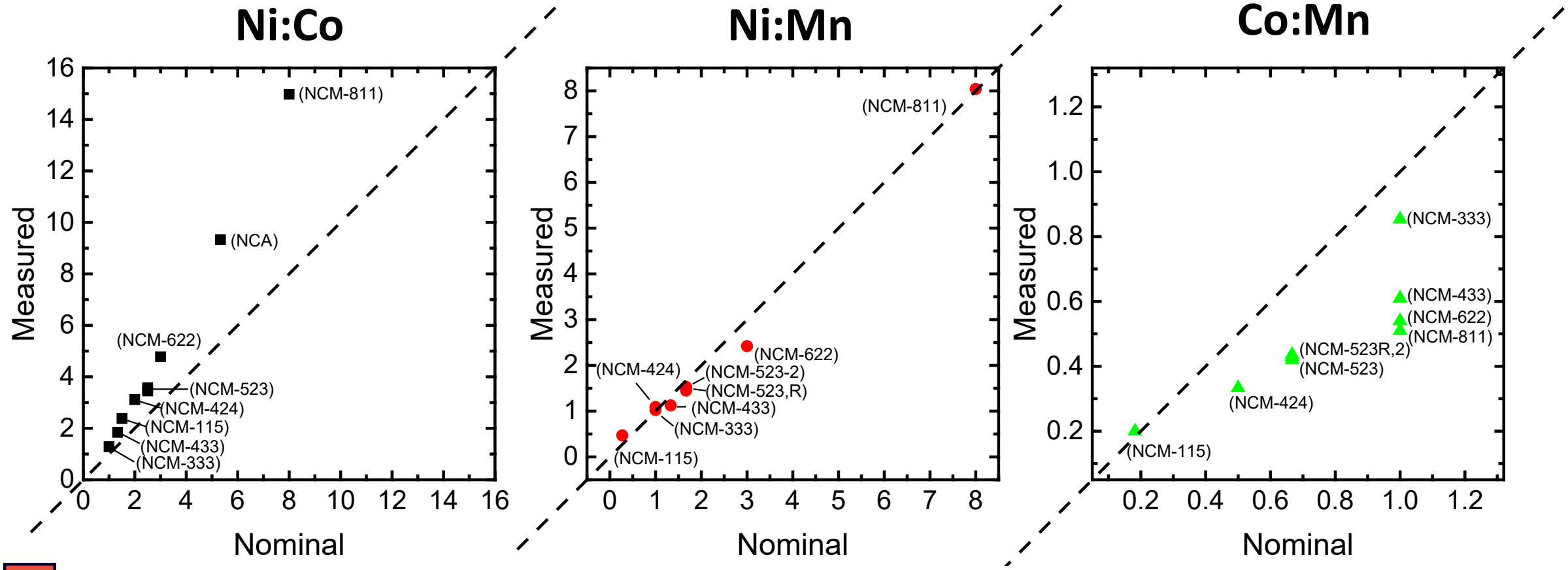

R. T. Haasch, S. E. Trask, D. P. Abraham, "Lithium-bearing oxides for rechargeable Li-ion batteries," *Surf. Sci. Spectra*, **26**, 014002 (2019). doi:10.1116/1.5080232.

Transition Metal Nitrides

First-Row Transition Metal Nitrides: ScN, TiN, VN, and CrN

XPS Analysis			ScN	TiN	VN	CrN
Binding energy (eV)	Metal $2p_{3/2}$	Major peak	400.4	455.1	513.2	574.4
		Satellite[a]		457.9	515.5	575.5
	Metal $2p_{1/2}$	Major peak	404.9	461.0	520.7	584.0
		Satellite[a]		463.8	523.0	585.1
	N 1s		396.1	397.3	397.0	396.7
Composition (N/metal)	As Deposited		1.13	1.00	1.02	0.73[b]
	After ion bombardment		0.99	0.73	0.46	0.55[b]
	Bulk value from RBS		1.11±0.03	1.02±0.02	1.06±0.02	1.04±0.02

a. The satellite is due to a transition into a relaxed final state
b. The composition determination of the CrN layers by peak fitting is less reliable because the commonly used Shirley method for background subtraction does not accurately describe the experimental data.

Nitrogen/Metal peak ratio decreases after sputtering

R. T. Haasch, T.-Y. Lee, D. Gall, C.-S. Shin, J. E. Greene, I. Petrov, *Surf. Sci. Spectra*, **7**, 169 (2000), *Surf. Sci. Spectra*, **7**, 193 (2000), *Surf. Sci. Spectra*, **7**, 221 (2000), *Surf. Sci. Spectra*, **7**, 250 (2000).

Layer Thickness Measurement

Layer thickness calculation: Two-Layer Model

Assuming only inelastic scattering

Beer-Lambert relationship:

$$I = I_0 \exp(-d/\lambda \cos\theta)$$

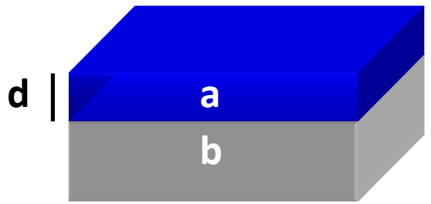

$$\frac{I_a}{I_b} \xrightarrow{\int} ln\left(\frac{N_a n_b \rho_b \lambda_b MW_a}{N_b n_a \rho_a \lambda_a MW_b} + 1\right) = \frac{d}{\lambda_a \cos\theta}$$

Where: η = number of atoms per molecule unit,
ρ = molecular density,
λ = inelastic mean-free path,
MW = molecular weight,
N = atomic concentration.

R. T. Haasch, "X-ray Photoelectron Spectroscopy (XPS) and Auger Electron Spectroscopy (AES)," in *Practical Materials Characterization*, M. Sardela, ed., (Springer Science + Business Media, New York, 2014). ISBN 978-1-4614-9280-1. doi: 10.1007/978-1-4614-9281-8_3.

Graphene Transfer

Layer-by-Layer Transfer of Multiple, Large Area Sheets of Graphene Grown in Multilayer Stacks on a Single SiC Wafer

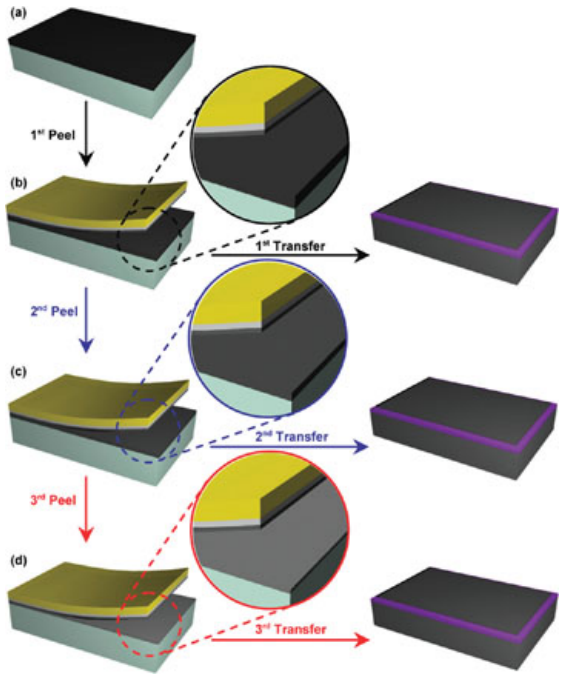

Graphene/SiC SiO_2

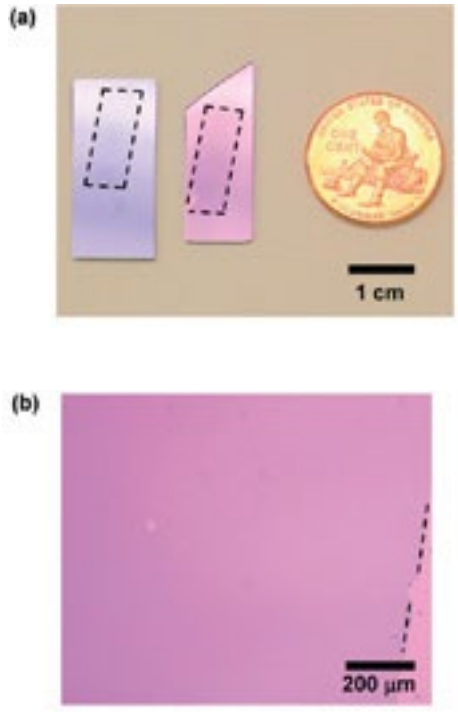

	Thickness, nm
As-grown	2.0
1st Transfer	1.5
2nd Transfer	0.8

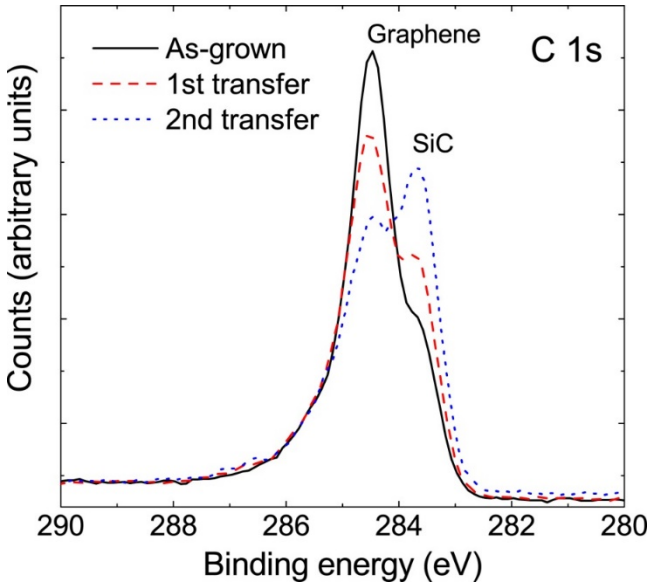

S. Unarunotai, J. Koepke, C.-L. Tsai, F. Du, C. Chialvo, Y. Murata, R. Haasch, I. Petrov, N. Mason, M. Shim, J. Lyding, J. A. Rogers, *ACS Nano*, **4(10)**, 5591-5598, (2010).

Angle-resolved XPS

More Surface Sensitive

θ = 75°

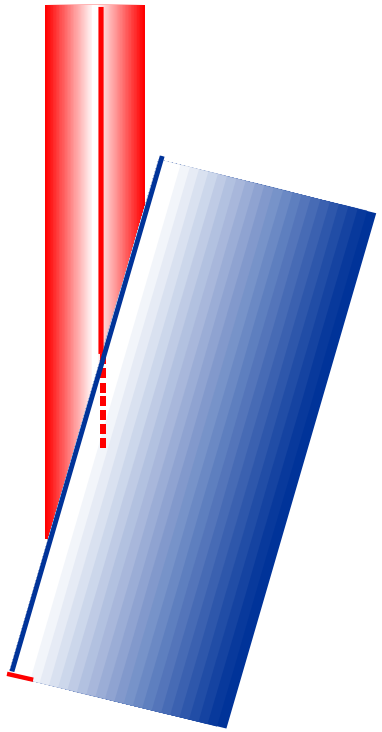

Less Surface Sensitive

θ = 0°

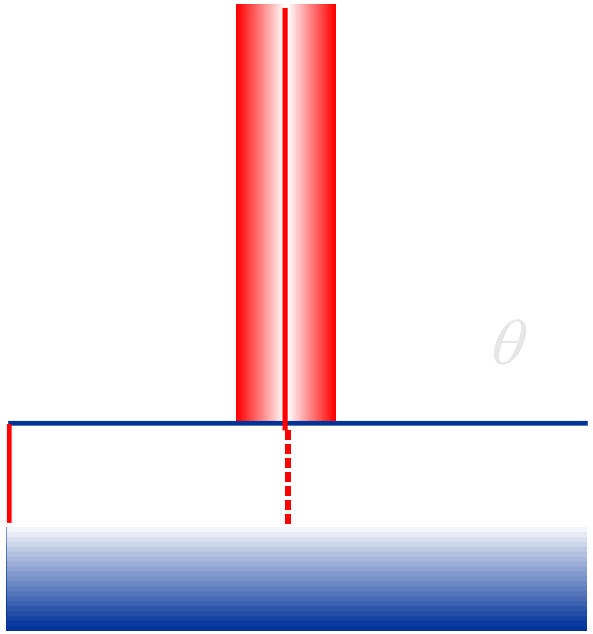

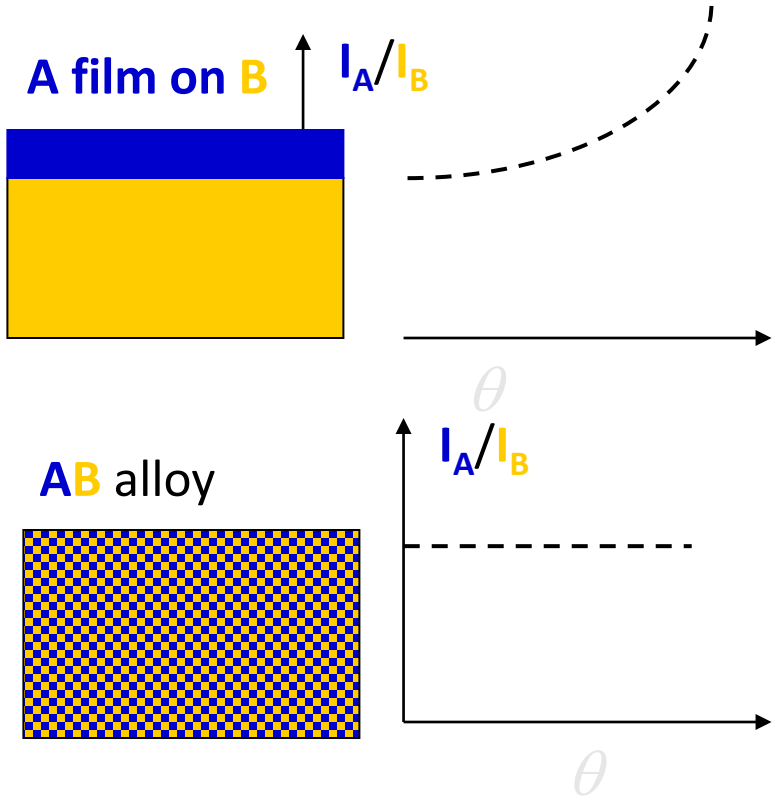

Information depth = dcosθ

d = Escape depth ~ 3 λ

θ = Emission angle (relative to surface normal)

λ = Inelastic Mean Free Path

Angle-resolved XPS - SiO_2/Si

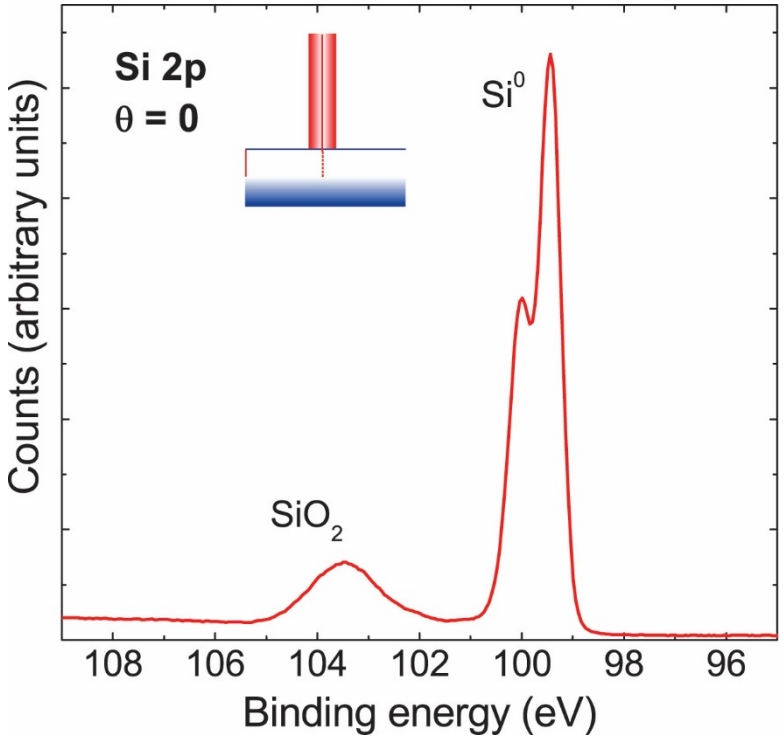

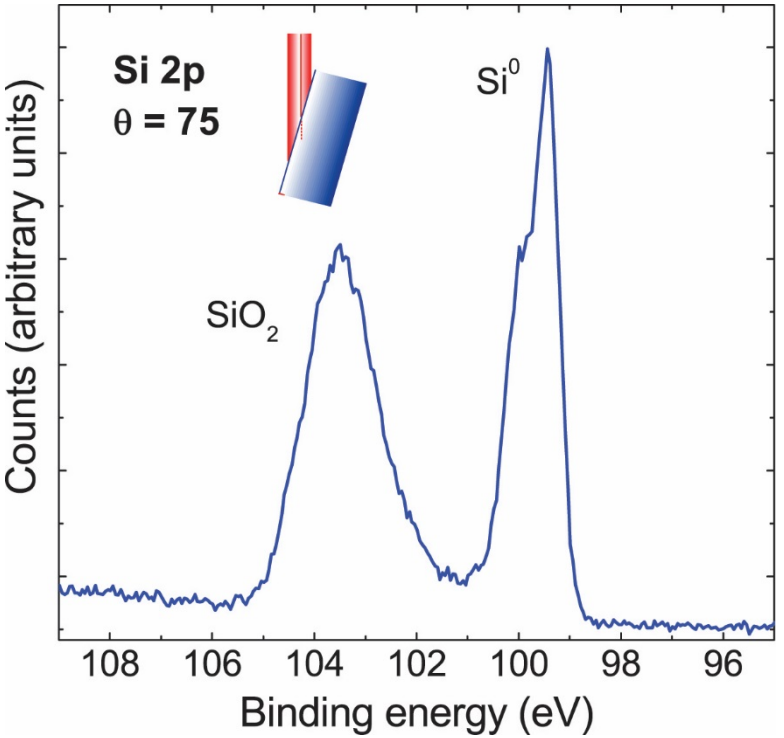

R. T. Haasch, "X-ray Photoelectron Spectroscopy (XPS) and Auger Electron Spectroscopy (AES)," in *Practical Materials Characterization*, M. Sardela, ed., (Springer Science + Business Media, New York, 2014). ISBN 978-1-4614-9280-1. doi: 10.1007/978-1-4614-9281-8_3.

Angle-resolved XPS - SiO_2/Si

Layer thickness calculation: Angle-resolved XPS

Beer-Lambert relationship:

$I = I_0 \exp(-d/\lambda \cos\theta)$

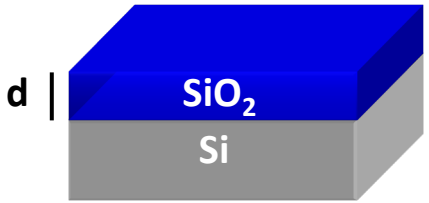

$$\frac{I_{SiO_2}}{I_{Si}} \quad \int \quad \rightarrow \quad ln\left(\frac{N_{SiO2}n_{Si}\rho_{Si}\lambda_{Si}MW_{SiO2}}{N_{Si}n_{SiO2}\rho_{SiO2}\lambda_{SiO2}MW_{Si}}+1\right)=\frac{d}{\lambda_{SiO2}\cos\theta}$$

Plot:

$$ln\left(\frac{N_{SiO2}n_{Si}\rho_{Si}\lambda_{Si}MW_{SiO2}}{N_{Si}n_{SiO2}\rho_{SiO2}\lambda_{SiO2}MW_{Si}}+1\right)=\frac{d}{\lambda_{SiO2}\cos\theta}$$

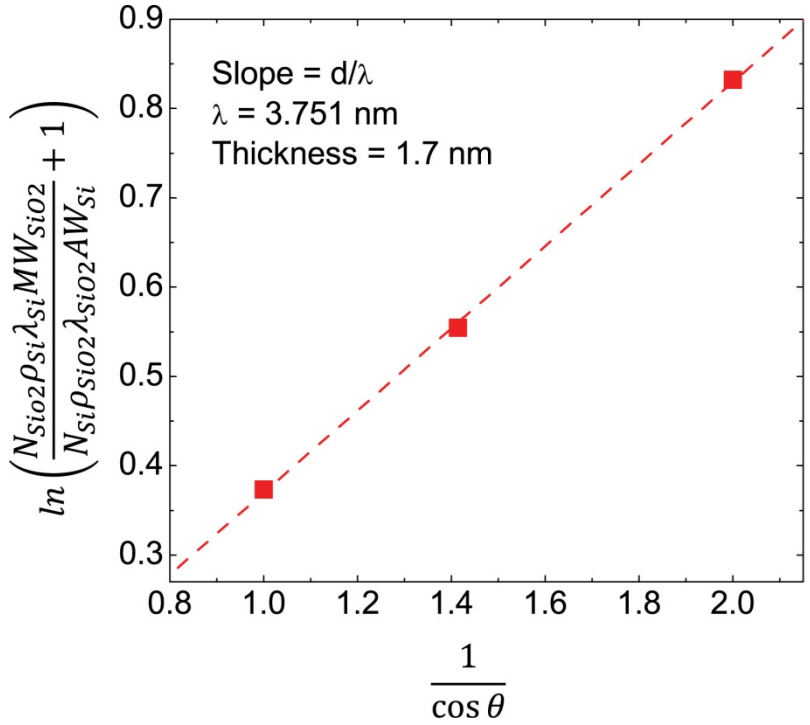

R. T. Haasch, "X-ray Photoelectron Spectroscopy (XPS) and Auger Electron Spectroscopy (AES)," in *Practical Materials Characterization*, M. Sardela, ed., (Springer Science + Business Media, New York, 2014). ISBN 978-1-4614-9280-1. doi: 10.1007/978-1-4614-9281-8_3.

XPS Imaging: Porous Silicon Pixel Array

Pt catalyzed etching of patterned porous silicon

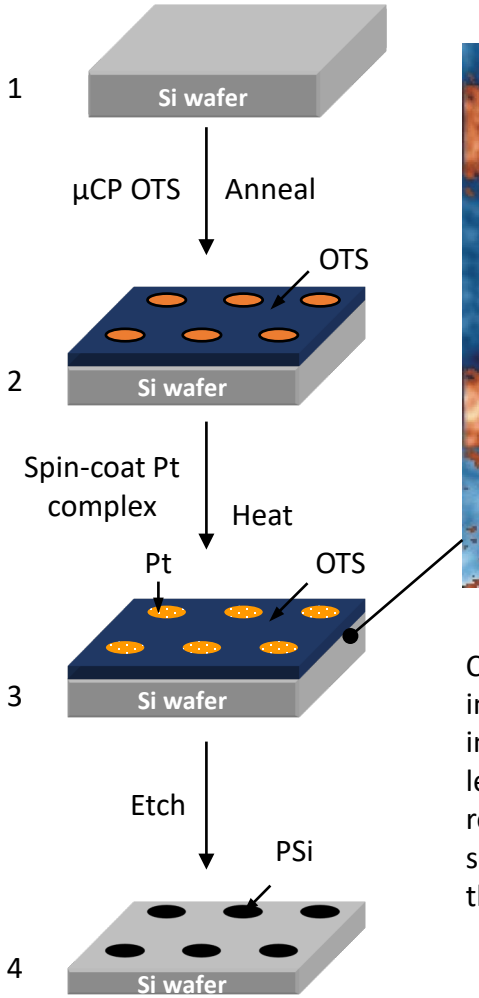

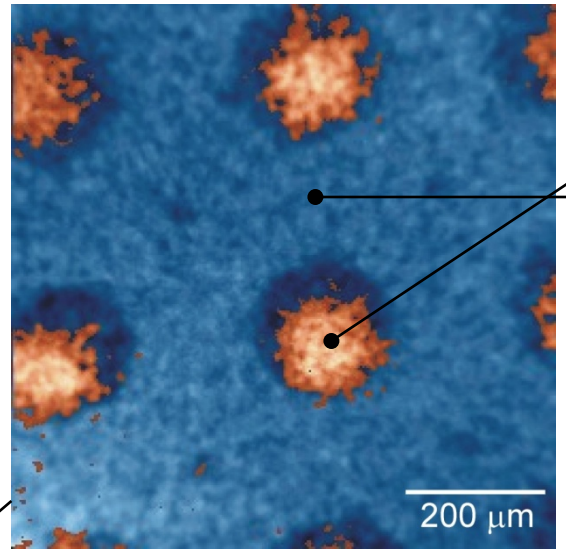

Cross-correlated, low-magnification XPS image after step 3 for the Pt $4f_{7/2}$ (shown in orange) and C 1s (shown in blue) core levels measured at 74 and 285 eV, respectively. The image confirms the selective deposition of the Pt-complex in the OTS-free areas of the substrate.

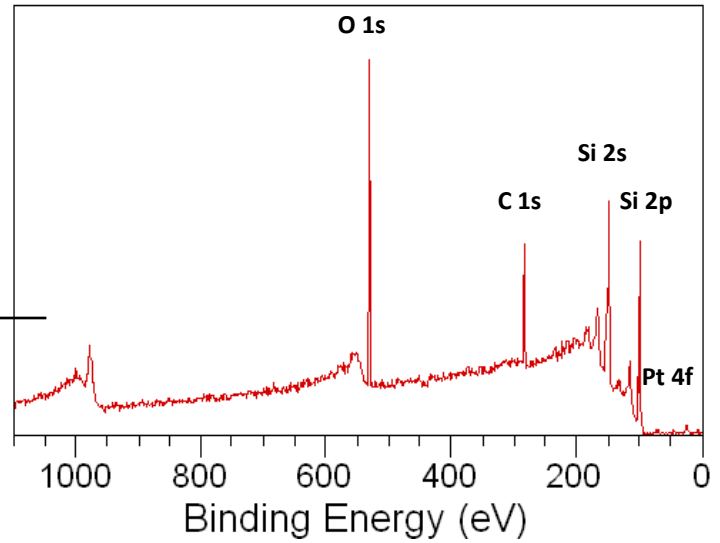

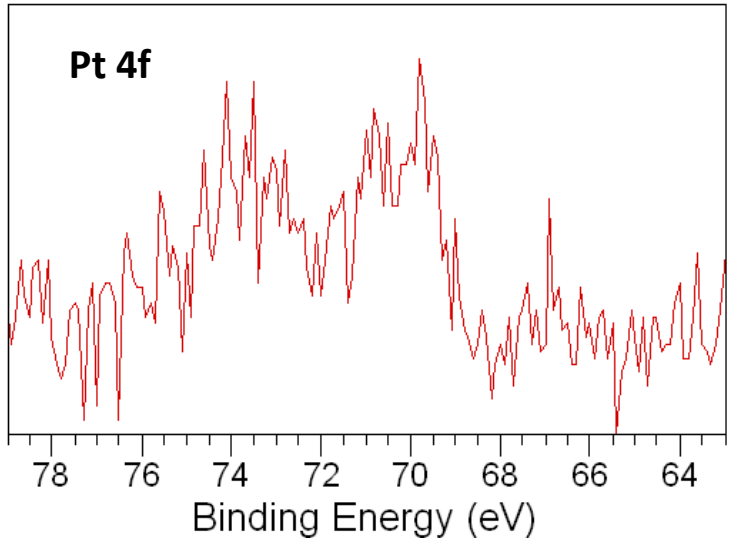

Y. Harada, X. Li, P. W. Bohn, R. G. Nuzzo, *JACS*, **123**, 8709-8717 (2001).

XPS Depth Profiling : LIB Solid-state Electrolyte

Monoatomic ion

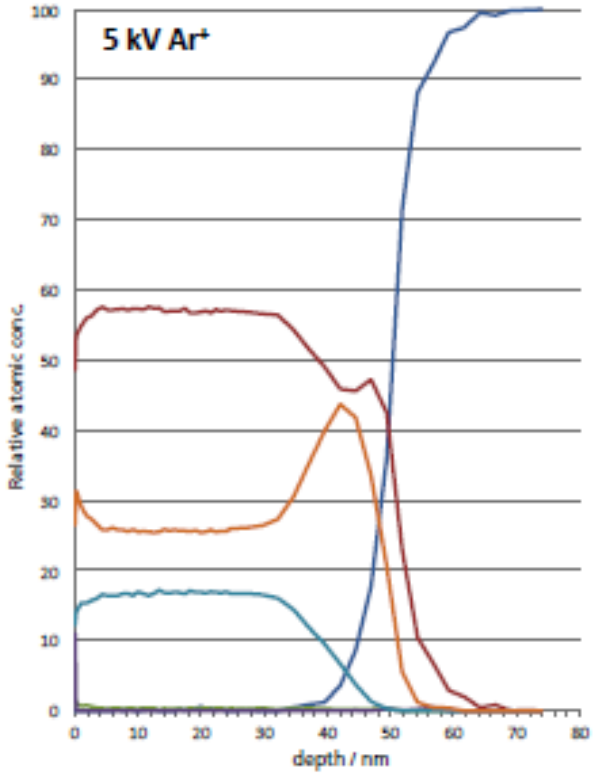

Figure 1(a) Sputter depth profile through ALD LiPON thin film using 5 keV Ar^+

Cluster ion

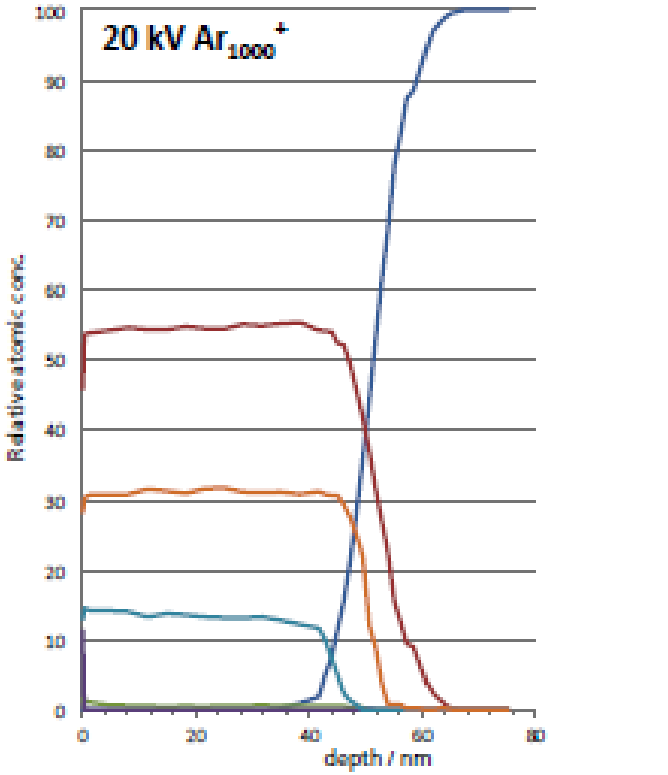

Figure 1(b) Sputter depth profile through ALD LiPON thin film using 20 keV Ar_{1000}^+

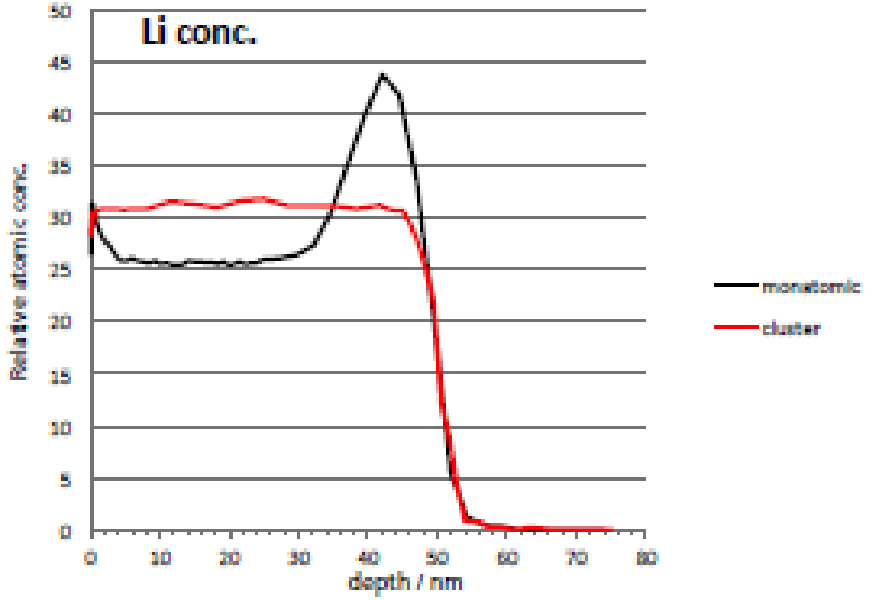

Figure 1(c) comparison of the Li concentration through the same sample generated using monatomic and cluster ion projectiles.

Image credit: https://www.kratos.com/

Technique Comparison: Resolution vs. Detection Limit

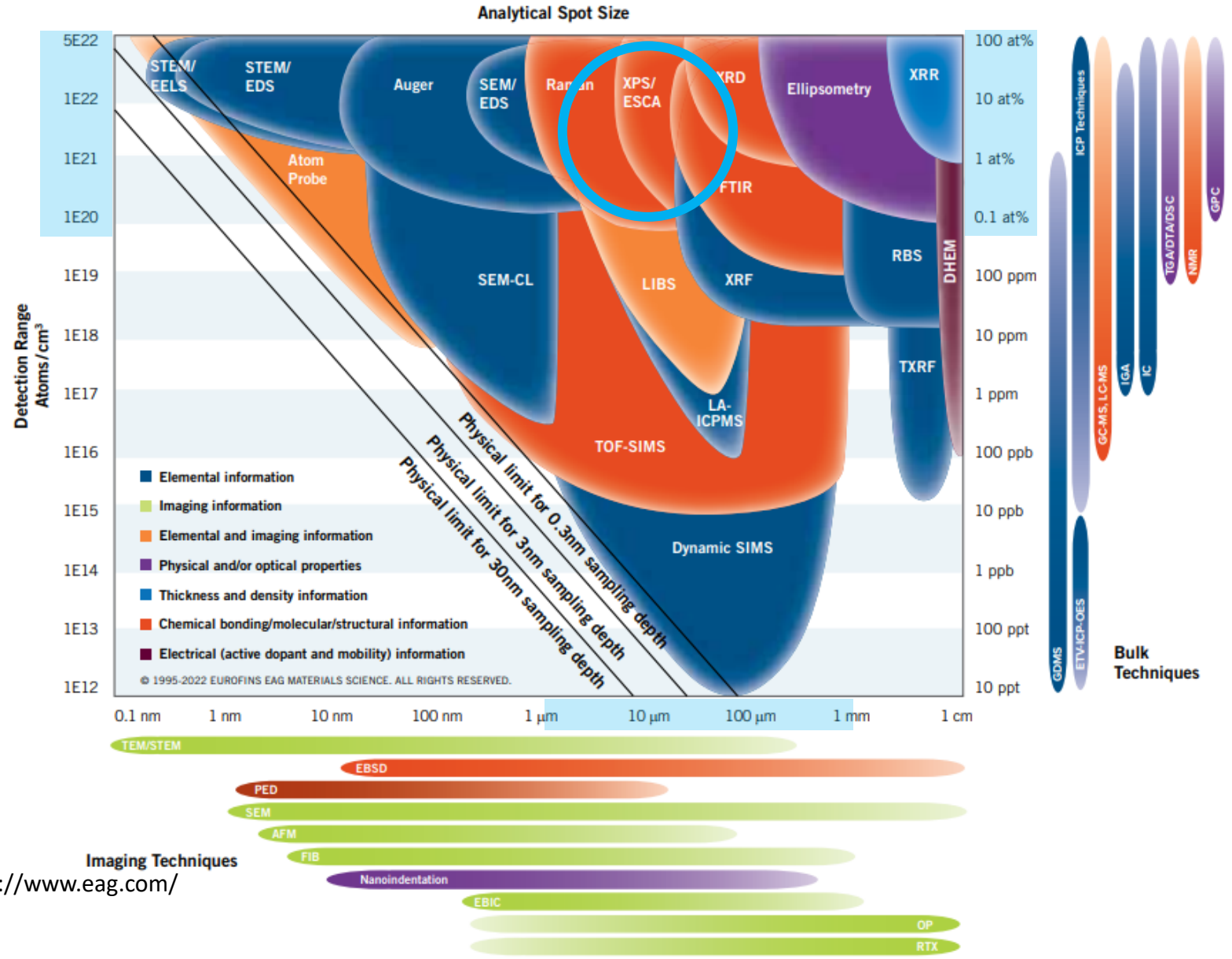

Image credit: https://www.eag.com/

Technique Comparison: Typical Analysis Depth

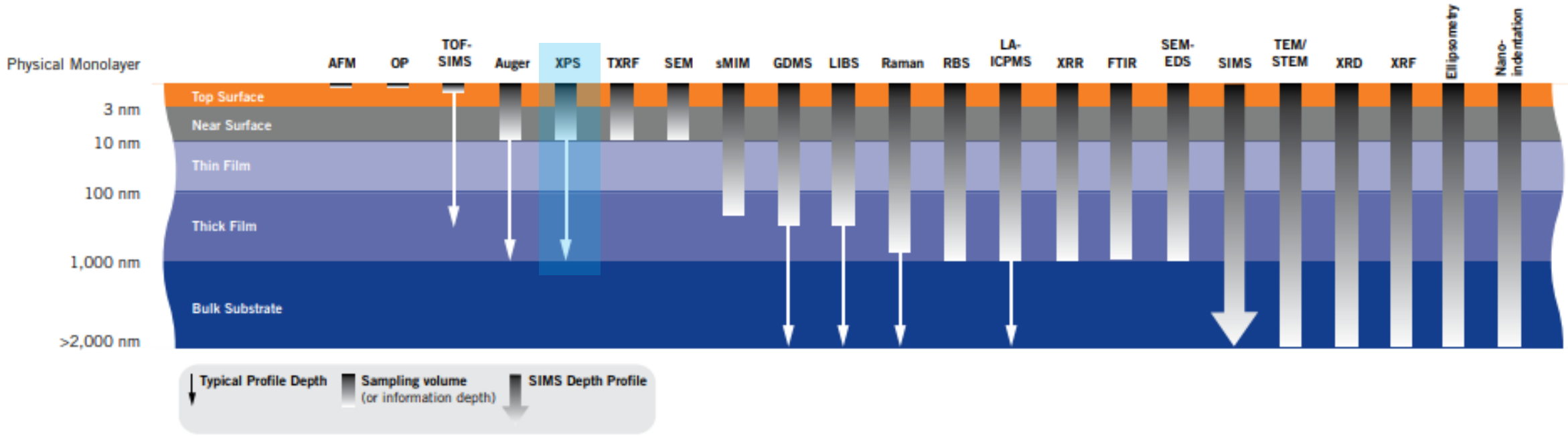

Image credit: https://www.eag.com/

Thank You to Our AMC 2024 Sponsors

Platinum sponsors:

Molecular Vista

Monstr Sense Technologies

NETZSCH Proven Excellence.

Oxford Instruments

Quantum Design

Surface Measurement Systems — World Leader in Sorption Science

ThermoFisher Scientific

Sponsors:

Angstrom Scientific Inc.

Anton Paar

Bruker

DMS D'Arcy Micro Sciences

Gatan + EDAX (AMETEK)

Hitachi — Inspire the Next

Horiba Scientific

JEOL Solutions for Innovation

Kratos Analytical — A Shimadzu Group Company

Kurt J. Lesker Company

nanoscribe — A BICO Company

Park Systems

PHCbi

Physical Electronics — A Division of ULVAC-PHI

samco — Partners in Progress

Thomas Scientific | Leica Microsystems

Waters™ | TA Instruments

ILLINOIS

Materials Research Laboratory

GRAINGER COLLEGE OF ENGINEERING